PERGAMON

Planetary and Space Science 47 (1999) 411–431

Planetary and Space Science

Geology of the Thaumasia region, Mars: plateau development, valley origins, and magmatic evolution

James M. Dohm, Kenneth L. Tanaka*

U.S. Geological Survey, 2255 North Gemini Drive, Flagstaff, Arizona, 86001, U.S.A.

Received 3 April 1998; received in revised form 16 October 1998; accepted 9 November 1998

Abstract

We have constructed the complex geologic history of the Thaumasia region of Mars on the basis of detailed geologic mapping and relative-age dating of rock units and structure. The Thaumasia plateau dominates the region and consists of high lava plains partly surrounded by rugged highlands, mostly of Noachian and Hesperian age. Long-lived faulting centered near Syria Planum and at lesser sites produced radiating narrow grabens during the Noachian through Early Amazonian and concentric wrinkle ridges during the Late Noachian and Early Hesperian. Fault activity peaked during the Noachian and waned substantially during Late Hesperian and Amazonian time. Volcanism on the Thaumasia plateau was particularly active in comparison with other martian cratered highlands, resulting in fourteen volcanoes and numerous outcrops of smooth, ridged, and lobate plains materials. A particularly extensive set of overlapping lava-flow units was emplaced sequentially from Thaumasia Planum to Syria Planum, spanning from the Late Noachian to the Late Hesperian; lobate flows succeeded smooth flow at the beginning of the Late Hesperian. Deep crustal intrusion and a thickened, buoyant crust may have caused the uplift of the plateau during the Noachian and Early Hesperian, resulting in outward-verging fold-and-thrust plateau margins. This structural style appears similar to that of the young ranges of the Rocky Mountains in the western U.S. Within the plateau, several sites of volcanotectonic activity and valley erosion may be underlain by large and perhaps long-lived magmatic intrusions. One such site occurs at the headland of Warrego Valles. Here, at least two episodes of valley dissection from the Noachian to Early Hesperian occurred during the formation of two nearby rift systems. The site also is a locus of intersection for regional narrow grabens during the Late Noachian and Early Hesperian. However, at the site, such faults diverge or terminate, which suggests that a resistant body of rock occurs there. The overall volcanotectonic history at Thaumasia fits into a model for Tharsis as a whole in which long-lived Syria Planum-centered activity is ringed by a few significant, shorter-lived centers of activity like the Thaumasia plateau. Valley formation, like tectonism in the region, peaked during the Noachian and declined substantially during the Hesperian and Amazonian. Temporal and spatial associations of single erosional valleys and valley networks with volcanoes, rift systems, and large impact craters suggest that the majority of valleys formed by hydrothermal, deformational, and seismic-induced processes. The origin of scattered, mainly Noachian valleys is more conjectural; possible explanations include local precipitation, seismic disturbance of aquifers, or unrecognized intrusions.

1. Introduction

The Thaumasia region (Fig. 1) is a major, complex volcanotectonic province of Tharsis for which comprehensive reconstruction of geologic history has been lacking. The region's topography and geology are unique to Tharsis and to the martian highlands. Unraveling Thaumasia's history, therefore, contributes to understanding the overall volcanotectonic history of Tharsis and the geologic processes that have affected highland cratered terrains. This undertaking is particularly vital since detailed structural histories of all other major tectonic provinces of Tharsis already have been derived from geologic and structural mapping, including Syria Planum and Noctis Labyrinthus (Tanaka and Davis, 1988), Tempe Terra and Ulysses Patera (Scott and Dohm, 1990b), Alba Patera (Tanaka, 1990), Valles Marineris (Witbeck et al., 1991), and Olympus Mons (Morris and Tanaka, 1994).

The Thaumasia region includes a tectonic plateau marked by interior high plains and surrounding ancient highlands. The highlands are fractured by Thaumasia, Claritas, Coracis, Melas, and Nectaris Fossae (Fig. 1). Within the highlands and parts of the interior plateau occur scattered massifs and volcanoes, mountain belts, numerous large impact craters, successions of lava-flow fields, and systems of rifts, narrow grabens, wrinkle ridges, and folds and thrusts. Erosion of rock materials

* Corresponding author. Tel.: 001 520 556 7208; fax: 001 520 556 7014; e-mail: ktanaka@flagmail.wr.usgs.gov

0032–0633/99/$ - see front matter
PII: S0032–0633(98)00141–X

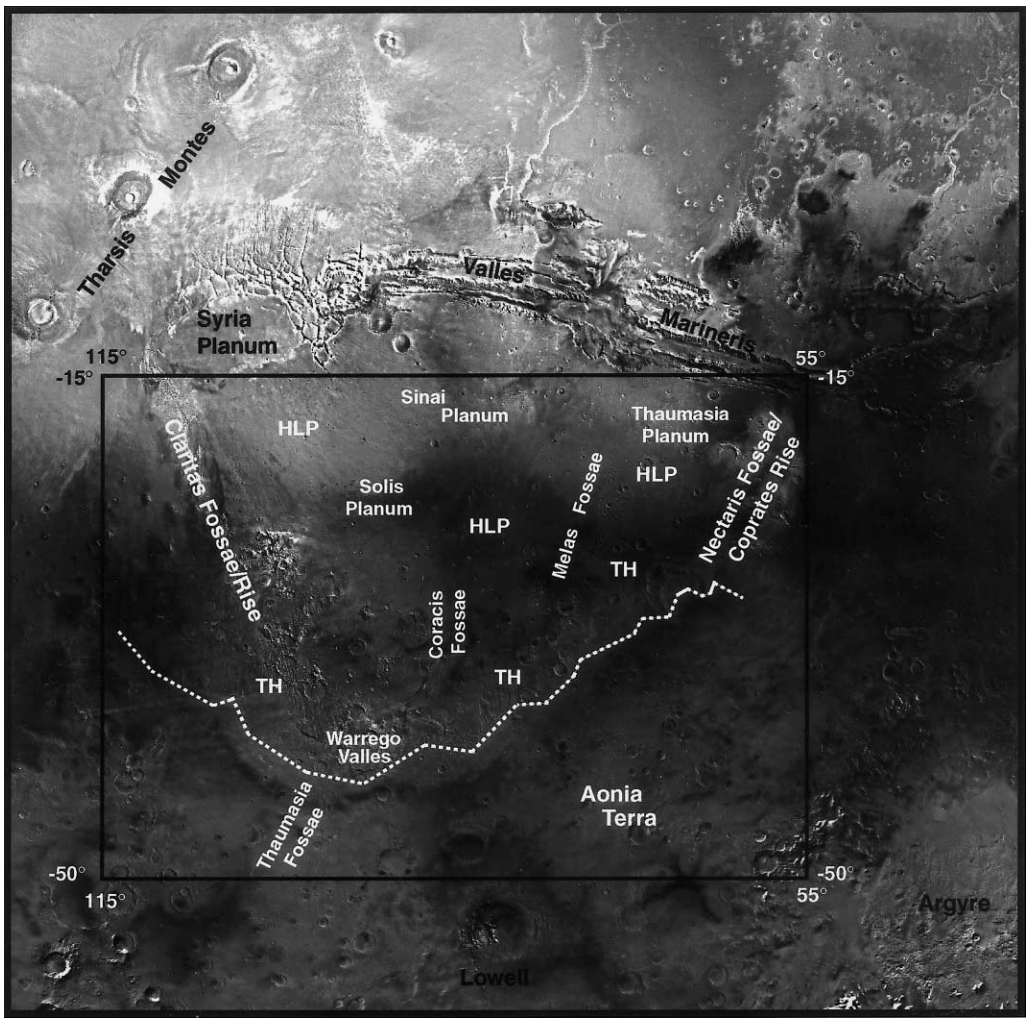

Fig. 1. Index map showing the Thausamia region (boxed area) of Mars. This region is dominated by the Thaumasia plateau (southern edge of plateau is dashed), which includes the high lava plains (HLP) of Syria, Sinai, Solis, and Thaumasia Plana and the partly surrounding Thaumasia Highland (TH) that is fractured by Thaumasia, Claritas, Coracis, and Nectaris Fossae and marked by mountain ranges (Coprates Rise, for example, is a mountain range that forms the eastern margin of the plateau).

and structures along parts of the outer margin of the Thaumasia plateau has resulted in extensive valley networks, canyons, troughs, and tilted, eroded rock layers forming cuestas (Saunders et al., 1980; Schultz and Tanaka, 1994). The relative ages and geologic relations of these features previously had been assessed only in local or broad-based studies (e.g., Wise et al., 1979; Scott and Tanaka, 1980, 1981, 1986; Plescia and Saunders, 1982; Scott and Dohm, 1990a; Tanaka et al., 1991; Schultz and Tanaka, 1994; Scott et al., 1995; Carr and Chuang, 1997).

Our study relies on a set of detailed rock-stratigraphic, paleotectonic, and paleoerosional maps of the Thaumasia region compiled at 1 : 5,000,000-scale (Dohm et al., in press) (Figs 2–4). Geologic units and tectonic and erosional structures were identified and mapped using medium- to high-resolution Viking images and 1 : 2,000,000-scale photomosaic bases. Our geologic data have been assembled into a Geographic Information System (GIS) database at 125-m resolution. Attributed characteristics for individual geologic features include type, size, and relative age. The database permits comparative analysis of spatial and temporal relations among rock units, topography, and erosional and tectonic structures. This paper consists of a general treatment of the map data; other studies provide more focused investigations of valley origin (Tanaka et al., 1998) and structural history (Anderson et al., 1997; Golombek et al., 1997).

2. Geologic setting

The Thaumasia study region (Fig. 1) consists of diverse rock materials, tectonic structures, and depositional and erosional landforms. The Thaumasia plateau dominates the region, extending $\sim$2,900 km across and rising more than 4 km above surrounding terrain. Significant features near this plateau include Valles Marineris, the north-

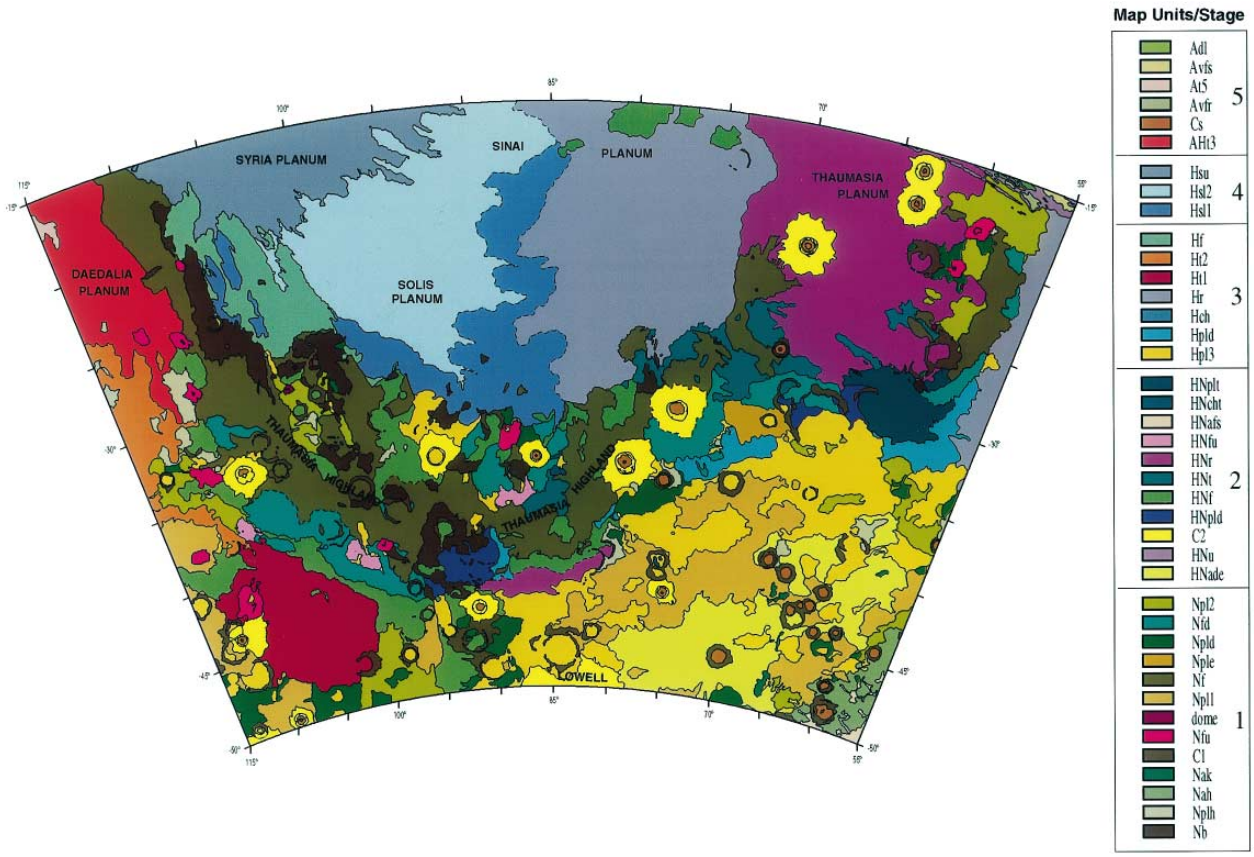

Fig. 2. Rock-stratigraphic map of the Thaumasia region of Mars (modified from Dohm et al., in press). Units shown grouped into five stages of geologic activity. Unit names given in Table 2, and stratigraphic position of stages relative to the martian stratigraphic system shown in Fig. 7.

western part of Argyre impact basin (in total ~1,500 km across and 2–3 km deep), the double-ring Lowell impact basin (200 km in diameter), and Syria Planum, near the center of the Tharsis rise. The northwest corner of the map area near the top of the Tharsis rise is at an elevation of > 8 km; the topography declines to Argyre Planitia in the southeast corner at < 4 km (U.S. Geological Survey, 1989). Plains areas that surround the Thaumasia plateau consist of ancient cratered terrain to the south, ridged plains to the east, and lobate lava plains of Daedalia Planum to the west.

We characterize the diverse geology of the Thaumasia region by distinguishing eleven geologic provinces (Fig. 5) based on their periods of geologic activity and their predominant geologic materials and structure, geomorphology, and gross topography (see Fig. 6). Such characteristics include fault and valley systems, highlands and massifs, various types of plains, volcanoes, broad canyons, and elevation ranges (Table 1).

3. Stratigraphy

The materials of the Thaumasia region have been divided into 39 geologic units based on stratigraphic relations and morphologic characteristics (Fig. 2) (Dohm et al., in press). We compiled crater statistics for 28 units having sufficient areal extent, which altogether cover 96.6% of the map region (Tables 2 and 3). These data were derived by counting all craters having rim diameters larger than 2 km and by calculating unit areas from our digital geologic map. Our data include populations of (1) total, or all identifiable craters, which at larger diameters reflect the emplacement ages of Noachian units, and (2) superposed craters only, which generally indicate the relative ages of Hesperian and Amazonian units and of resurfacing for Noachian units. Some complex units formed over multiple stages of development, such as the Noachian/Hesperian dissected units that consist of older cratered material partly resurfaced by valley erosion and associated sedimentation.

To assess relative age ranges among unit outcrops and how they might vary by geographic region, we produced and analyzed crater counts of individual outcrops and of outcrops grouped according to local to regional physiographic associations. Our crater-density data are summarized in Table 3, which include time-stratigraphic unit assignments using the scheme of Tanaka (1986). In addition, our mapping (Dohm et al., in press) indicates

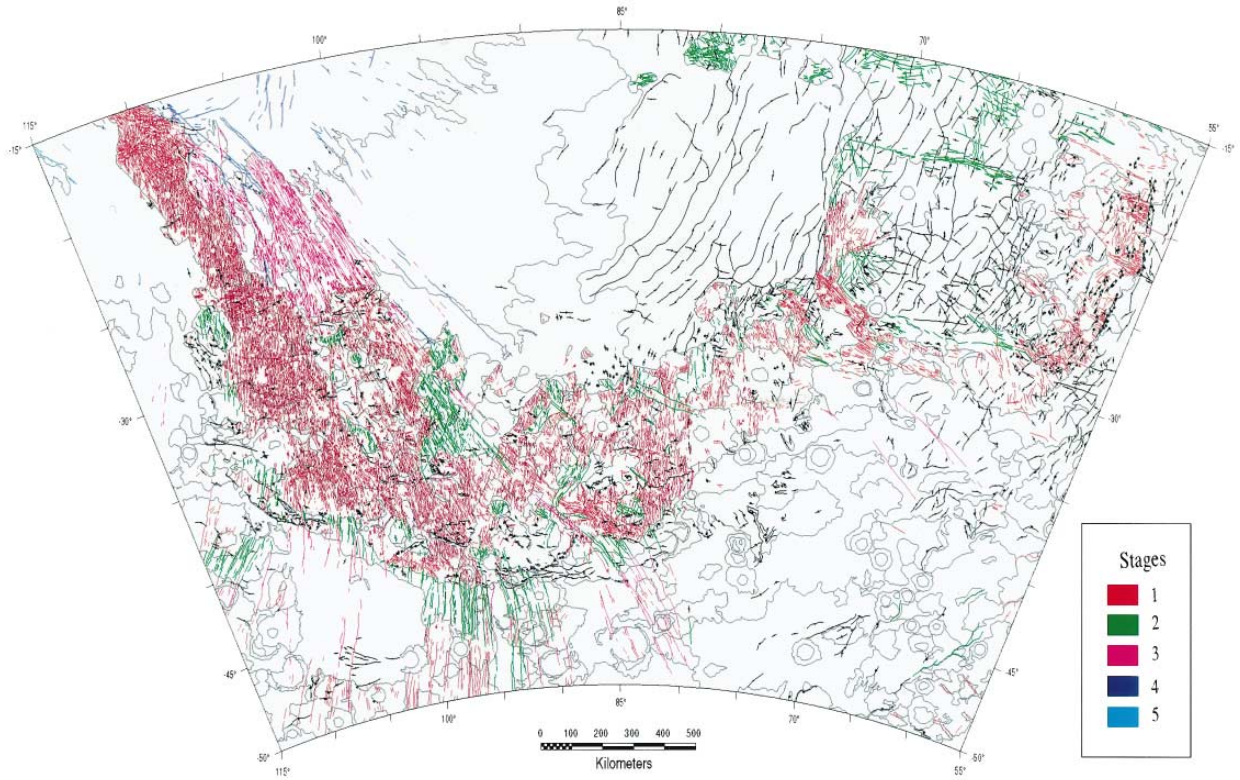

Fig. 3. Paleotectonic map of the Thaumasia region of Mars (modified from Dohm et al., in press). Fault and graben development shown by geologic stage; also shown are scarps and ridges (black lines) and rock-unit boundaries (gray lines).

five main stages of geologic activity in the Thaumasia region to which each map unit was assigned (see Figs 2 and 7 and Table 2). We conservatively show some overlap in the age ranges of these stages based on water-density constraints (Fig. 7). These stages roughly correspond the martian stratigraphic scheme (Tanaka, 1986) as follows: stage 1, Noachian; stage 2, Late Noachian to Early Hesperian; stage 3, Early Hesperian; stage 4, Late Hesperian to Early Amazonian; stage 5, Amazonian.

We summarize the rock-stratigraphic history of the Thaumasia region, from oldest to youngest rocks (based on Dohm et al., in press; see Fig. 2 and Table 2), as follows. The oldest rock units (stage 1) consist of ancient, heavily cratered rocks that form plateaus, rugged mountains and hills, prominent ridges, and highly degraded crater rims. Complex modification of these ancient rock units due to cratering, tectonic deformation, erosional processes (including valley formation), and volcanic and sedimentary burial has degraded or destroyed older craters, making it difficult to constrain the onset of unit formation. Thus the morphology of stage 1 units is commonly dominated by features that postdate the emplacement of the material. More resistant materials making up the early crust apparently form the local massifs and mountain ranges common on the Thaumasia plateau and the rim material of the Argyre impact basin. Less rugged plateau and plains rocks that in many areas intermingle with or partly bury the more rugged units may consist of mixtures of impact breccias, volcanic materials, and eolian, colluvial, and fluvial sediments. For example, the Argyre impact likely produced a thick blanket of ejecta that makes up much of the stage 1 units surrounding the basin; much of the ejecta is probably reworked. Fourteen mountains on and west of the plateau, many of which have summit depressions, highly dissected flanks, and (or) flank flows, occur along or near fault systems (Fig. 8); in agreement with some previous work (Scott and Tanaka, 1981, 1986), we interpret these to be volcanic edifices. However, uplift associated with basin formation also has been suggested as a mechanism for some of these features (Schultz et al., 1982; Craddock et al., 1990).

Our stratigraphic data indicate that the more rugged units mostly formed during stage 1 (Fig. 2 and Table 2), whereas lower relief units and the volcanic constructs formed throughout stages 1 and 2. The extensive older ridged plains material (unit HNr), which covers much of Thaumasia Planum, forms a distinctive stratigraphic marker for stage 2. Some materials have been heavily modified by faulting and (or) valley development during stage 2; these units are assigned a stage 2 age, although

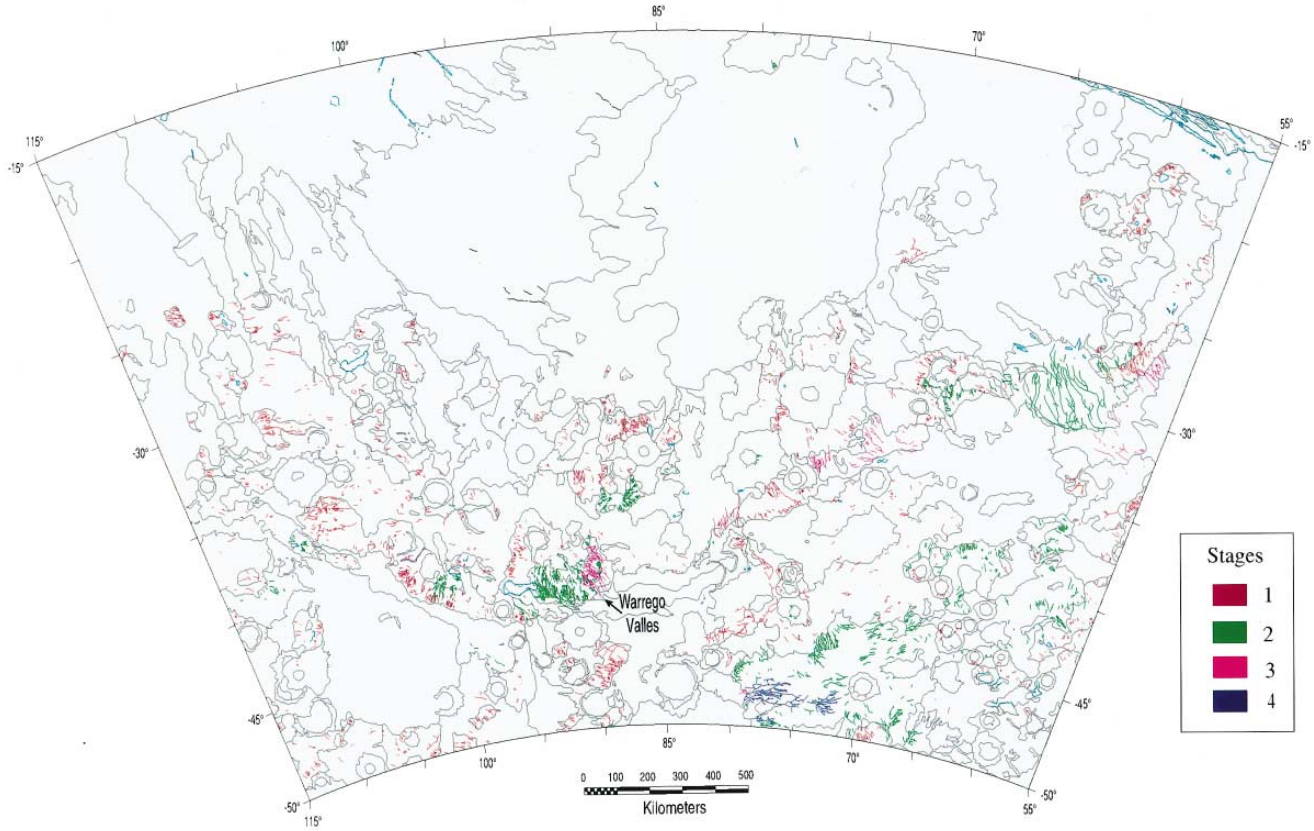

Fig. 4. Paleoerosional map of the Thaumasia region of Mars (modified from Dohm et al., in press). Valley development shown by geologic stage, as well as depressions (dark blue lines) and lava rilles (black lines), relative to contacts of geologic units (gray lines).

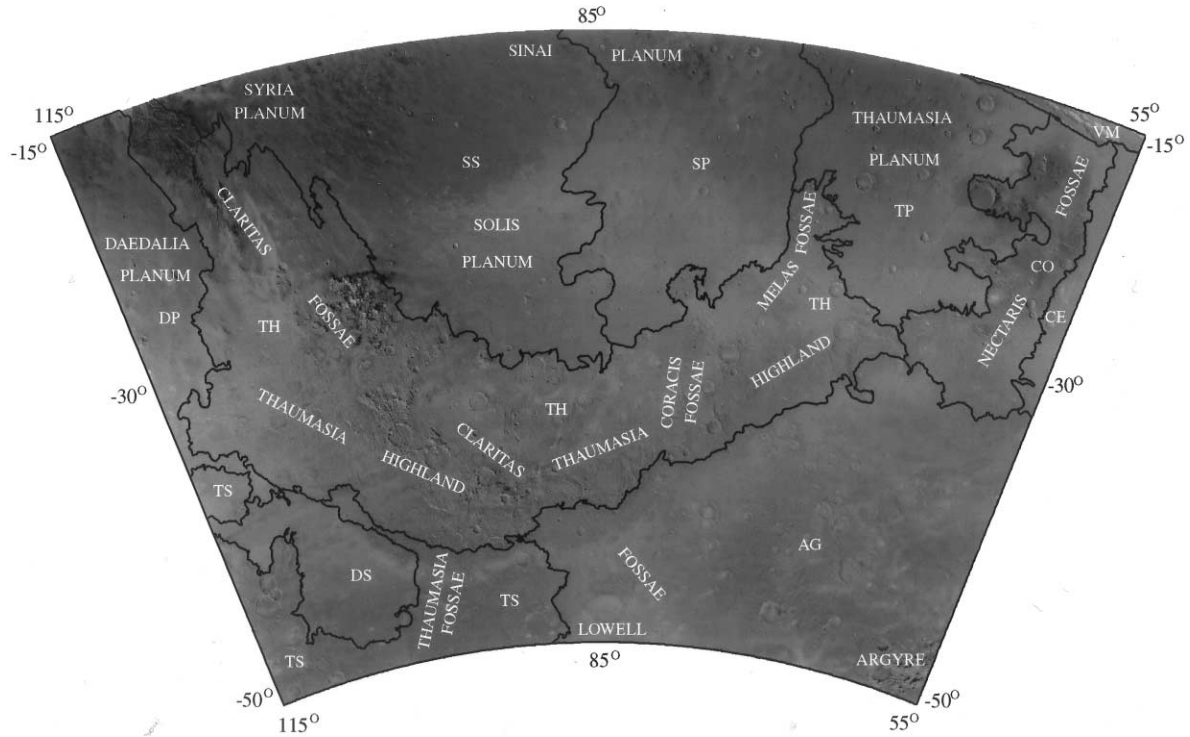

Fig. 5. Photomosaic of the Thaumasia region showing major physiographic provinces, as follows: Thaumasia Highlands (TH), Daedalia Planum (DP), Syria–Solis Plana (SS), Terra Sirenum (TS), Daedalia Southeast (DS), Thaumasia Planum (TP), Coprates (CO), Sinai Planum (SP), Argyre (AG), Coprates East (CE), and Valles Marineris (VM).

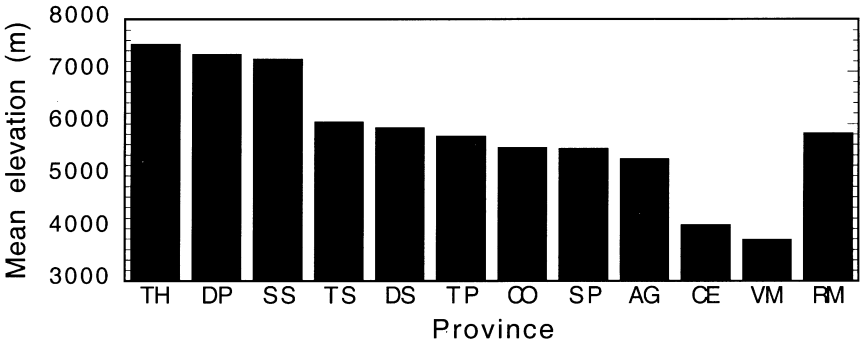

Fig. 6. Histogram showing mean elevations for each physiographic province (see Fig. 5) relative to the regional mean elevation (RM) for all of Thaumasia.

Table 1
Principal landforms and their relative ages for major physiographic provinces of the Thaumasia region of Mars

Province name	Symbol	Relative age*	Major landforms
Valles Marineris	VM	LN–H	Deep rifts and collapse structures
Coprates East	CE	EH	Ridged plains
Coprates	CO	N–EH	Cratered terrain, broad ridges, tilted rock layers, wrinkle ridges, narrow grabens, rift systems; depressions, valleys and troughs, volcanoes
Thaumasia Planum	TP	LN–EH	Ridged plains, sets of narrow grabens
Sinai Planum	SP	EH	Ridged plains
Syria–Solis Plana	SS	LH	Lobate flows, sparse narrow grabens
Thaumasia Highlands	TH	N–H	Narrow graben and rift systems, broad ridges, tilted rock layers, volcanoes, smooth plains, valleys and troughs
Daedalia Planum	DP	EH–A	Lobate flows, massifs, volcanoes, sparse grabens
Daedalia Southeast	DS	EH	Smooth plains, narrow grabens, subdued wrinkle ridges
Terra Sirenum	TS	N–EH	Cratered terrain, narrow grabens, valleys, volcanoes
Argyre	AG	N–EH	Cratered and smooth plains, plateaus, basins, valleys, subdued ridges

*N = Noachian, H = Hesperian, A = Amazonian, E = Early, L = Late.

parts of the outcrops likely include stage 1 rock surfaces. Rock materials of stages 1 and 2 cover more than half of the Thaumasia region (Tables 4 and 5).

Stage 3 records extensive ridged plains volcanism in the Sinai Planum and Coprates East provinces of the Thaumasia region, as well as local valley formation and deposition along parts of the southern margin of the Thaumasia plateau. Extensive stages 3 and 4 sheet lavas in the Syria-Solis, Daedalia Planum, and Daedalia Southeast provinces were erupted from the crest and flanks of Syria Planum and of the Tharsis Montes volcanoes. Rock materials of stages 3 and 4 make up over 40% of the Thaumasia region (Tables 4 and 5). Stage 5 materials, which mainly consist of relatively small outcrops of volcanic materials and colluvial and eolian deposits, represent about 3% of the total rock outcrop in the Thaumasia region.

We also used our stratigraphic results to constrain the relative ages of tectonic structures and valleys relative to the five stages defined by our geologic mapping (Dohm et al., in press; Figs 3 and 4). Relative ages were determined by crosscutting relations between features and the rock units. Our age-dating methods were similar to those used to unravel the structural histories of the Syria Planum (Tanaka and Davis, 1988), Tempe Terra and Ulysses Patera (Scott and Dohm, 1990b), and Alba Patera (Tanaka, 1990) regions of Mars.

We digitized the mapped tectonic and erosional features and their relative-age assignments into a GIS database to perform statistical calculations. We determined the number of faults and valleys and total fault and valley lengths per stage in the map region (Table 5). Additionally, we calculated for each stage the areal extent of rock outcrops within each physiographic province (Fig. 9) and the fault-, wrinkle ridge-, and valley-length densities (Figs 10–12). These data indicate the relative intensity of structural deformation and valley erosion in space and time for the Thaumasia region.

4. Tectonic history

The history of tectonic events in the Thaumasia region is recorded in part by the distribution and ages of fault and ridge systems (Fig. 3). We have mapped and dated over 15,000 tectonic structures, which include faults and

Table 2
Unit symbols, unit names, number of outcrops, area, and geologic stage (see Fig. 7)

Unit symbol	Unit name	Number of outcrops	Area (km^2)	Stage
Nb	Basement complex	50	163,520.66	1
Nplh	Hill unit	26	53,490.47	1
Nah	Basin-rim unit, Argyre	3	44,673.36	1
Nak	Knobby unit, Argyre	6	5428.28	1
C_1	Material of degraded craters	106	144,935.14	1
Nfu	Older flow and construct material	11	41,666.11	1
Dome	Domes	9	2277.65	1
Npl_1	Cratered unit	20	356,138.03	1
Nf	Older fractured material	23	608,851.60	1
Nple	Etched material	2	21,553.51	1
Npld	Older dissected material	32	119,135.38	1
Nfd	Fractured and dissected material	17	208,912.34	1
Npl_2	Subdued cratered unit	25	206,419.71	1
HNade	Dissected and etched unit, Argyre	6	254,601.78	2
HNu	Undivided material	7	11,913.14	2
C_2	Material of fresh to subdued craters	13	202,011.21	2
HNpld	Intermediate dissected material	4	41,925.51	2
HNf	Intermediate fractured material	41	281,392.23	2
HNt	Terraced material	13	95,991.25	2
HNr	Older ridged plains materials	4	437,188.19	2
HNfu	Younger flow and construct material	3	18,890.31	2
HNafs	Smooth floor unit, Argyre	4	9826.13	2
HNcht	Chaotic material	5	2691.62	2
HNplt	Troughed material	2	64,196.69	2
Hpl_3	Smooth unit	73	492,460.03	3
Hpld	Younger dissected material	4	75,091.87	3
Hch	Channel and flood-plain material	3	626.49	3
Hr	Younger ridged plains material	3	623,334.36	3
Ht_1	Member 1, Tharsis Montes Fm	1	183,840.68	3
Ht_2	Member 2, Tharsis Montes Fm	2	92,782.97	3
Hf	Younger fractured material	5	122,488.61	3
Hsl_1	Older flows of lower member, Syria Planum Fm	5	279,312.62	4
Hsl_2	Younger flows of lower member, Syria Planum Fm	3	435,357.16	4
Hsu	Upper member, Syria Planum Fm	1	210,500.46	4
AHt_3	Member 3, Tharsis Montes Fm	1	165,599.36	5
C_s	Smooth crater floor material	26	27,644.22	5
Avfr	Rough floor material, Valles Marineris	1	1613.78	5
At_5	Member 5, Tharsis Montes Fm	1	4132.81	5
Avfs	Smooth floor material, Valles Marineris	6	3030.68	5
Adl	Linear dune material	1	451.43	5

Note: The areas of the final geologic map shown here (from Dohm et al., in press) vary slightly from the areas derived from a preliminary geologic map used in the crater data in Table 3.

grabens, mare-type wrinkle ridges, and broad and narrow ridges (Dohm et al., in press).

Although the relative ages of a few individual faults may not be well constrained, our approach treats those faults as belonging to fault systems of generally consistent orientation, morphology, and relative age. For example, Claritas Fossae (Figs 3 and 8) consist of a complex system of graben and fault segments. Narrow grabens that are wholly confined to Noachian host rocks follow a narrow range of trends and are assigned to stage 1. However, it cannot be determined if some of the individual fault segments were formed or reactivated after stage 1. But we infer that few such younger faults exist, because a much greater density of faults in stage 1 rocks vs younger units in this area is observed.

4.1. Regional tectonism

Our analysis of Thaumasia's faults and grabens, rift systems, and wrinkle ridges (Fig. 3) indicate that tectonic activity began and reached its peak during the Noachian (stage 1) and declined during the Hesperian and Amazonian periods (stages 2–5; Table 5). These results are in general agreement with previous works (Tanaka, 1986; Scott and Dohm, 1990a) but provide more temporal, spatial, and geologic detail. Additionally,

Table 3
Cumulative crater densities and unit ages of geologic units in the Thaumasia region of Mars

Unit symbol	Area (km^2)	Type[3]	Average crater density[1] N(2)	[Crater age[2]] N(5)	N(16)	Unit age[2]
AHt_3	166,759	t	408 ± 50 [LH–EA]	84 ± 22 [LH–EA]		LH–EA
		s	366 ± 47 [LH–EA]	42 ± 16 [EA]		
Hsu	210,309	t	585 ± 53 [LH]	95 ± 21 [LH]	5 ± 5 [EH]	LH
		s	580 ± 53 [LH]	90 ± 21 [LH]	5 ± 5 [EH]	
Hsl_2	436,307	s	504 ± 34 [LH]	53 ± 11 [EA]	7 ± 4 [EH]	LH
Hsl_1	281,560	t	583 ± 46 [LH]	114 ± 20 [EH–LH]	11 ± 6 [EH]	LH
		s	579 ± 45 [LH]	110 ± 20 [EH–LH]	11 ± 6 [EH]	
Hf^n	115,972	t	543 ± 68 [LH]	95 ± 29 [LH–EA]	9 ± 9 [EH]	LH
Ht_2	92,680	t	701 ± 87 [EH–LH]	194 ± 46 [LN–EH]	43 ± 22 [LN–EH]	EH
		s	669 ± 85 [EH–LH]	162 ± 42 [LN–LH]	43 ± 22 [LN–EH]	
Ht_1	194,508	t	694 ± 60 [EH–LH]	113 ± 24 [EH–LH]	15 ± 9 [EH]	EH
		s	663 ± 58 [LH]	82 ± 21 [LH–EA]	10 ± 7 [EH]	
Hpld	74,247	s	1037 ± 118 [EH]	148 ± 45 [EH–LH]		EH
Hr	632,513	t	694 ± 33 [LH]	161 ± 16 [EH]	25 ± 16 [LN–EH]	EH
		s	672 ± 33 [LH]	139 ± 15 [EH–LH]	19 ± 6 [LN–EH]	
Hpl_3	500,602	t	1125 ± 47 [EH]	210 ± 21 [LN–EH]	22 ± 7 [LN–EH]	EH
		s	1075 ± 46 [EH]	160 ± 18 [EH]	12 ± 5 [EH]	
HNplt	64,627	s	851 ± 115 [EH–LH]	139 ± 46 [EH–LH]	16 ± 16 [LN–EH]	LN–EH
HNafs	9805	t	1122 ± 338 [N–EH]	306 ± 177 [MN–EH]		LN–EH
		s	1020 ± 323 [N–LH]	204 ± 144 [LN–EA]		
HNpld	45,912	t	1481 ± 180 [N]	305 ± 82 [LN]	22 ± 22 [LN–EH]	LN–EH
		s	1285 ± 167 [N–EH]	109 ± 49 [EH–EA]		
HNr	496,792	t	968 ± 44 [EH]	213 ± 21 [LN–EH]	28 ± 8 [LN–EH]	LN–EH
HNt	87,864	t	1081 ± 111 [EH]	285 ± 57 [LN]	34 ± 20 [LN–EH]	LN–EH
		s	1059 ± 110 [EH]	262 ± 55 [LN]	34 ± 20 [LN–EH]	
HNf	270,407	t	1010 ± 61 [EH]	266 ± 31 [LN]	48 ± 13 [LN]	LN–EH
		s	958 ± 60 [EH]	215 ± 28 [LN–EH]	33 ± 11 [LN–EH]	
HNade	254,890	t	1146 ± 67 [N–EH]	369 ± 38 [MN–LN]	63 ± 16 [LN]	LN–EH
		s	891 ± 59 [EH]	118 ± 22 [EH–LH]	12 ± 7 [EH]	
HNfc	18,919	t	1480 ± 280 [N–EH]	317 ± 130 [MN–EH]	53 ± 53 [MN–EH]	LN–EH
		s	1269 ± 259 [N–EH]	106 ± 75 [EH–EA]		
Npl_2	218,561	t	1606 ± 86 [N]	545 ± 50 [MN]	124 ± 24 [MN–LN]	MN–LN
		s	1299 ± 77 [N]	238 ± 33 [LN]	46 ± 15 [LN]	
Nfd	212,311	t	1437 ± 82 [N]	325 ± 39 [LN]	99 ± 22 [MN–LN]	MN–LM
Npld	112,824	t	1675 ± 122 [N]	541 ± 69 [MN]	124 ± 33 [MN–LN]	MN–LN
		s	1365 ± 110 [N]	239 ± 46 [LN–EH]	18 ± 13 [LN–EH]	
Nple	22,416	t	1606 ± 268 [N]	491 ± 148 [EN–LN]	178 ± 89 [EN–LN]	MN–LN
		s	1338 ± 244 [N–EH]	223 ± 100 [LN–LH]		
Nf	630,233	t	1453 ± 48 [N]	424 ± 26 [MN–LN]	108 ± 13 [MN–LN]	EN–LN
Nfc	40,406	t	2203 ± 234 [N]	569 ± 119 [EN–MN]	99 ± 50 [MN–LN]	EN–LN
Npl_1	430,909	t	1673 ± 62 [N]	610 ± 38 [EN–MN]	202 ± 22 [EN–MN]	EN–MN
Nb	168,733	t	2157 ± 113 [N]	581 ± 59 [EN–MN]	190 ± 34 [EN–MN]	EN–MN
Nah	54,551	t	1027 ± 137 [EH]	568 ± 102 [EN–MN]	202 ± 61 [EN–MN]	EN–MN
Nplh	59,638	t	2733 ± 214 [N]	989 ± 129 [EN]	335 ± 75 [EN]	EN–MN

[1] Average crater density N(D) equals number of craters larger than diameter D per million square kilometers.
[2] Relative ages based on time-stratigraphic scale from Tanaka (1986) and reflect material ages, which include stratigraphic relations (see text); N = Noachian, H = Hesperian, A = Amazonian, E = Early, M = Middle, and L = Late. In a few instances, crater age varies from unit age because of varying amounts of statistical error.
[3] Type of crater count; superposed (s) and total (t), which includes superposed and highly eroded, partly buried impact craters. For Noachian units, type t more reflects material age; for younger units, type t often indicates underlying material age. Type s reflects emplacement or resurfacing age. Not all units have both types of data, because some units only have superposed craters, whereas superposed craters could not be consistently distinguished from others on the oldest Noachian units.

the intense extensional and contractional deformation of the Thaumasia region appears to have largely resulted from (1) Tharsis- and Syria-centered volcanotectonic activity (stages 1–5), (2) uplift and associated rifting of the Thaumasia plateau (mainly stages 1 and 2), which includes local centers of volcanotectonic activity, and (3) formation and tectonic relaxation of the Argyre impact basin (stages 1 and 2) (Dohm et al., in press).

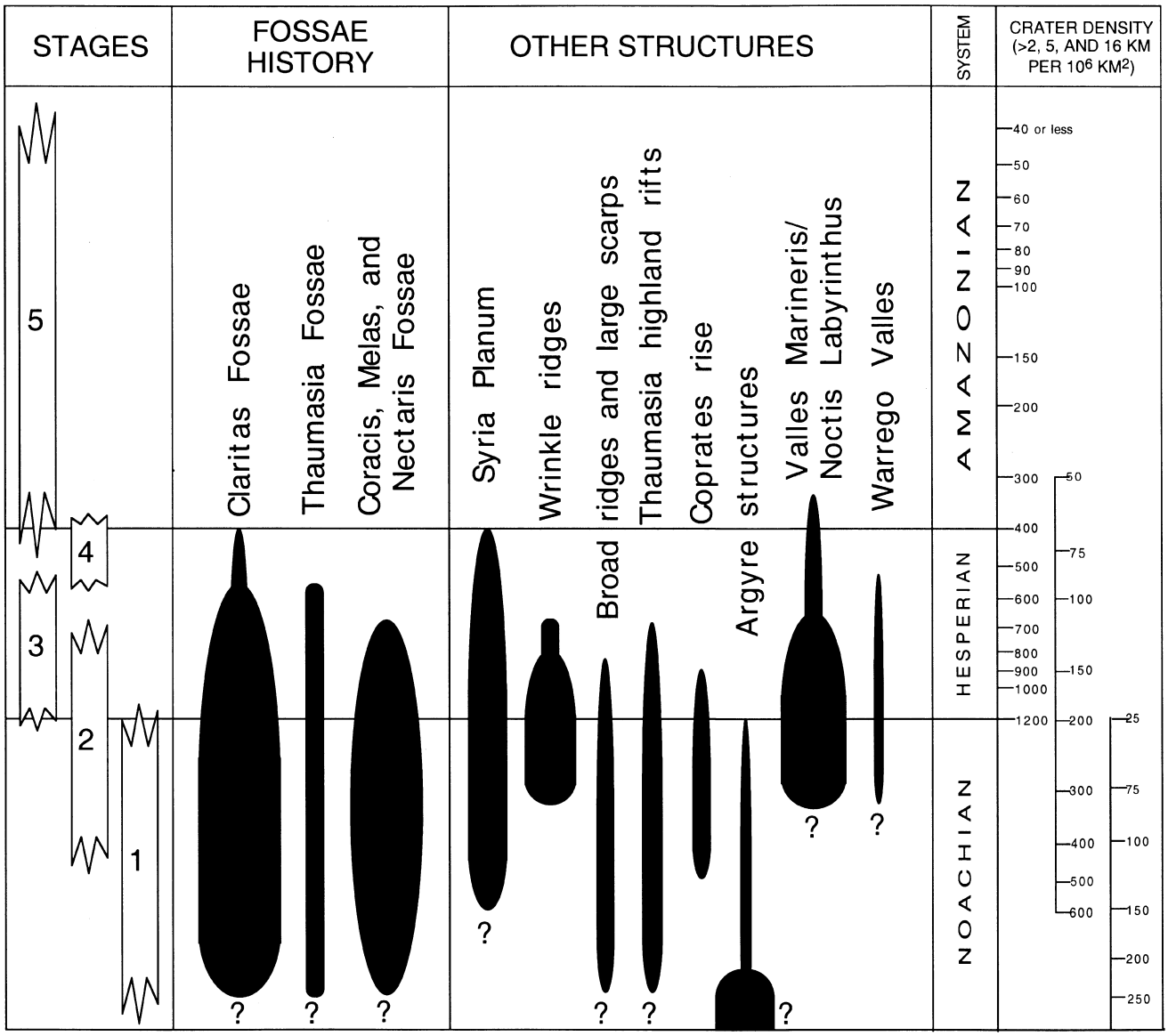

Fig. 7. Chart comparing the stages of geologic activity in the Thaumasia region with major sets of tectonic structures. Size of solid areas roughly proportional to degree of exposed deformation; question marks indicate where uncertainty exists in the commencement of structural activity. Crater chronology from Tanaka (1986).

Table 4
Area of map region covered by rocks of each major stratigraphic period

Period	Area (km^2)
Noachian	3,397,630
Hesperian	2,681,394
Amazonian	36,872

Note: Noachian includes Noachian/Hesperian units and Hesperian includes Hesperian/Amazonian units

Other stress sources may have contributed to the tectonic deformation of the region, such as compression due to rapid planetary cooling (e.g., Tanaka et al., 1991).

4.2. Tharsis- and Syria-centered tectonic activity

Claritas Fossae radiate from Tharsis and form the densest and most numerous system of faults and grabens in Thaumasia (Fig. 7). Prolonged extensional tectonism (stages 1–4) resulted in the formation, and subsequent reactivation, of narrow (< 5 km across) and wide (> 5 km across) grabens. Thaumasia Fossae in the southwest corner of the map region (Figs 1 and 3) apparently formed a southern extension of Claritas Fossae during stages 1–3. Faulting at Claritas commenced during the Early to Middle Noachian (stage 1), declined during Late Noachian and Early Hesperian (stages 2 and 3), and substantially diminished during Late Hesperian/Amazonian (stages 4 and 5). An observed significant change from

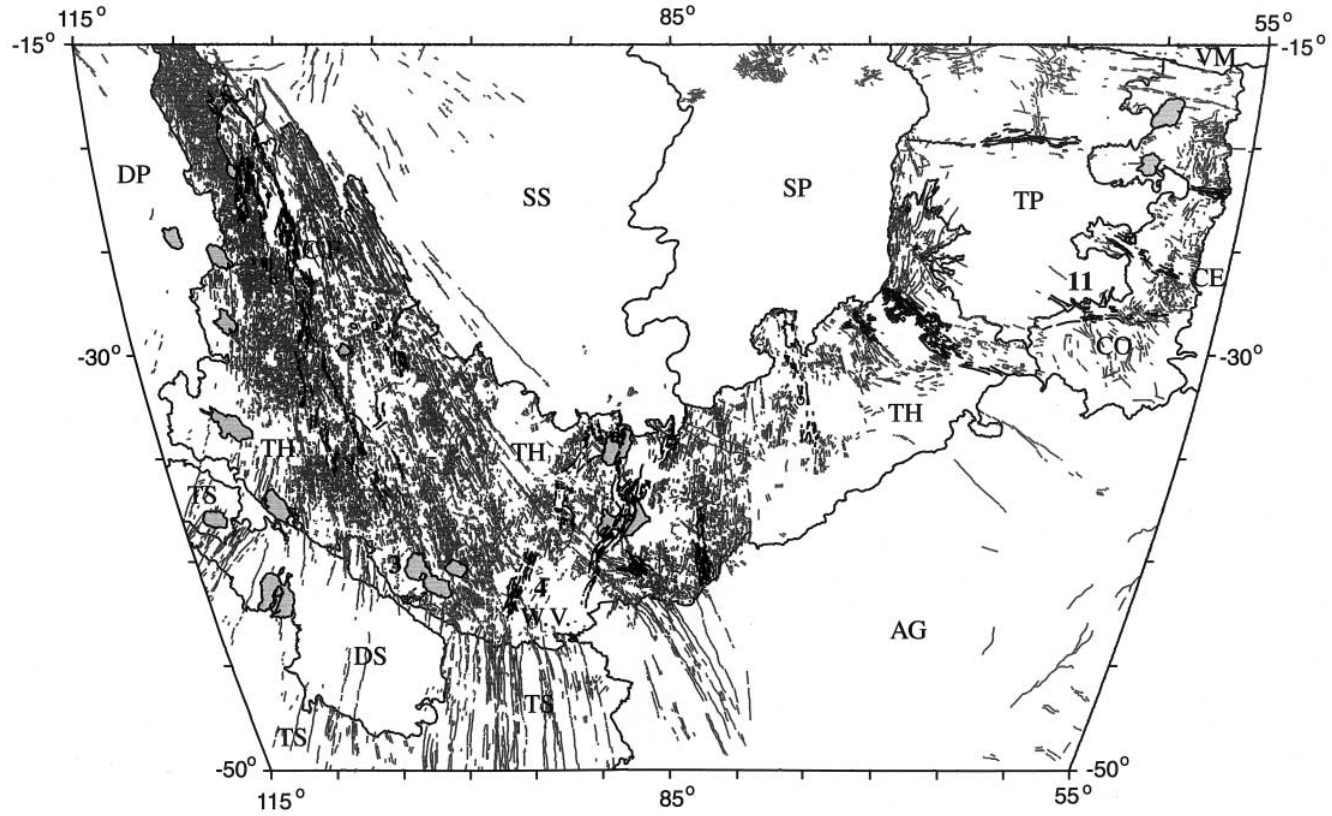

Fig. 8. Map showing geologic provinces of the Thaumasia region (black lines and letter symbols defined in Fig. 5). Note spatial correlations among provinces, faults and grabens (dark gray lines), volcanoes (light gray areas), and rift systems (black lines) (see Fig. 3 for more fault detail). Special features of interest include Claritas Fossae (CF) and Warrego Valles (WV). Rift nos 3, 4, and 11 represent best candidate sites of intrusive activity (also see corresponding Fig. 13).

Table 5
Area of outcrops, number of faults and valleys, and total fault and valley lengths for each stage in the Thaumasia region

Stage	Area (km^2)	Number of faults	Number of valleys	Total fault length (km)	Total valley length (km)
1	1,977,002	10,620	3105	161,045	26,509
2	1,420,628	2043	1928	42,320	20,584
3	1,590,625	1196	469	28,153	4697
4	925,170	174	0	5670	0
5	202,472	14	1	316	9

tectonic to volcanic Tharsis-dominated activity during the Late Hesperian in the Thaumasia region, which includes a decline in Tharsis-radial normal faulting, may coincide with a decline in intrusive thickening of the crust at Tharsis (Tanaka et al., 1991).

Other significant tectonic structures occur mainly in the Thaumasia Planum and Coprates provinces (Fig. 3), including grabens that are radial to and parallel with Valles Marineris. These structures cut stage 1 and 2 rock materials in the Sinai Planum, Thaumasia Planum, Coprates, and Thaumasia Highlands provinces but are buried by stage 3 younger ridged plains material (unit Hr) of the Sinai Planum province. Some of these structures may be related to the formation of Valles Marineris, including stage 2 faults that are radial to and concentric about the south-central part of Valles Marineris (Anderson et al., 1998; Dohm et al., 1998). These relations indicate a sharp decline of Tharsis- and Syria-centered normal faulting during the Early to later Hesperian for the northeastern part of the Thaumasia region.

Additionally, Late Noachian/Early Hesperian (stages 2 and 3) Syria-centered activity produced wrinkle ridges in the Sinai Planum, Thaumasia Planum, and Coprates East provinces. Wrinkle ridges formed before and after emplacement of the younger ridged plains unit (unit Hr;

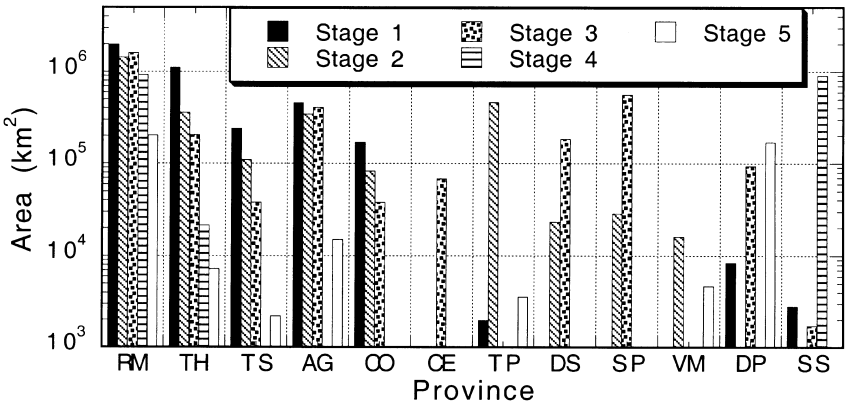

Fig. 9. Histograms representing the amount of rock units per stage for each province (Fig. 5) and for the regional mean (RM) within the Thaumasia region.

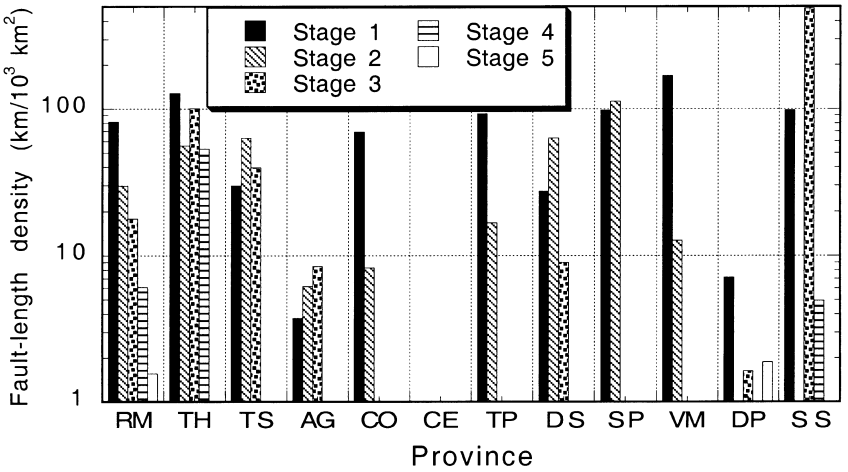

Fig. 10. Histograms representing the areal density of fault length per stage for each province (Fig. 5) and for the regional mean (RM) within the Thaumasia region.

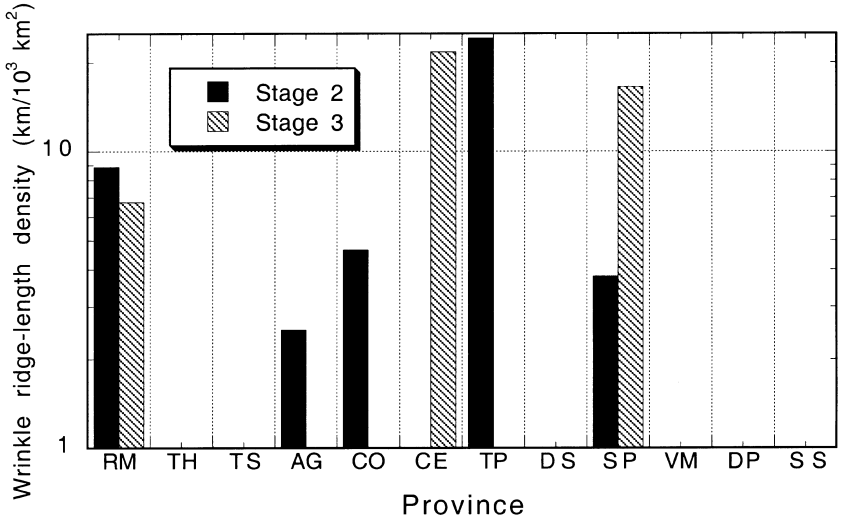

Fig. 11. Histograms representing the areal density of wrinkle ridge length per stages 2 and 3 for each province (Fig. 5) and for the regional mean (RM) within the Thaumasia region.

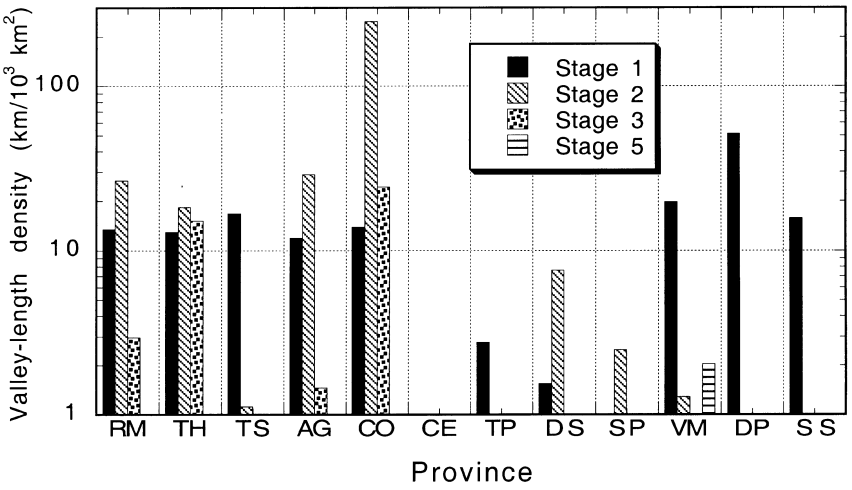

Fig. 12. Histograms representing the areal density of valley length per stages 1–3 and 5 for each province (Fig. 5) and for the regional mean (RM) within the Thaumasia region.

Fig. 2), suggesting that wrinkle-ridge development occurred over a long time span. Syria Planum, active as a volcanotectonic center from Noachian to perhaps Early Amazonian (Tanaka and Davis, 1988; Tanaka et al., 1996), includes the following features: (1) a raised north rim; (2) dense stage 1–3 concentric and radial grabens; and (3) stage 4 lavas that buried Syria Planum's southeast rim and stages 3 and 4 lavas that infill the planum interior. Scattered extensional structures surrounding Syria Planum reactivated or formed after the emplacement of the voluminous stage 4 sheet lavas, including nearby concentric and radial grabens, collapse troughs of Noctis Labyrinthus, and grabens within Valles Marineris (Witbeck et al., 1991). Only minor Tharsis-related faulting occurred in the Daedalia Planum province during stage 5 (Early Amazonian).

4.3. *Argyre impact-related tectonic deformation*

The Argyre impact event excavated a broad, deep basin and produced structurally controlled scarps, broad ridges, valleys, and mountain ranges within several hundred kilometers of the basin margin and oriented radial and concentric to the basin. Stages 1 and 2 isostatic adjustments after the basin formation (Thomas and Masson, 1984; Wichmann and Schultz, 1989) may have resulted in the production of many of the geologic features. Near the Thaumasia plateau, lower-relief basins and broad rises may in part have resulted from Argyre-related deformation (Craddock et al., 1990). Some 2000 km away from the basin, the outline of the southeast margin of the Thaumasia plateau is roughly concentric with Argyre basin, suggesting that the margin could be controlled by impact-related crustal structure (Fig. 1).

5. Volcanic history

The Thaumasia region preserves some of the best examples of early highland volcanoes and intermediate-age plateau lavas on Mars. Their evolution may provide clues to regional and perhaps global magmatic evolution as well. Many of the prominent, isolated mountains within the Coprates, Thaumasia Highlands, Daedalia Planum, and Terra Sirenum provinces occur along or near faults and commonly exhibit summit depressions and highly dissected flanks. They have been interpreted by most workers as ancient volcanoes (Saunders et al., 1980; Scott and Tanaka, 1981, 1986; Witbeck et al., 1991; Hodges and Moore, 1994); we have mapped fourteen such features as possible volcanoes. In addition to morphology, we note that their stratigraphic relations indicate that they are not the oldest rocks of the plateau. Thus, they are not likely to be massifs of ancient impact basins, as suggested by Craddock et al. (1990) or other ancient crustal material, as interpreted by Scott and King (1984). Furthermore, many of the constructs formed along extensional fault systems having similar ages, suggesting a correlation between their formation and active tectonism (Fig. 8). Similar to the rift systems, many of these fault-controlled constructs appear to have developed over long periods of time.

Stratigraphic relations and crater counts for the volcanoes (Fig. 2 and Table 3) suggest that they formed throughout most of the Noachian and into the Early Hesperian. Stages 1 and 2 of volcano construction have been delineated on the geologic map (Fig. 2). Unlike the Hesperian to Amazonian, large shield volcanoes on Mars that display extensive lobate flows such as Olympus Mons and the Tharsis Montes (e.g., Plescia and Saunders, 1979; Greeley and Spudis, 1981; Scott, 1982), the complex mor-

phologies of the Thaumasia volcanoes may indicate interbedded lavas and pyroclastic deposits (Scott and Tanaka, 1981). Thus early volcanism in the Thaumasia region may have been in part explosive, perhaps as a result of volatile-rich magmas or of the interaction of magma and ground water or ice. Similar origins have been considered for highly dissected, Noachian/Early Hesperian paterae-type volcanoes elsewhere on Mars that are believed to comprise pyroclastic deposits such as Hecates Tholus and Tyrrhena, Hadriaca, and Apollinaris Paterae (Reimers and Komar, 1979; Mouginis-Mark et al., 1982; Greeley and Crown, 1990; Crown and Greeley, 1993; Robinson et al., 1993). Another possibility is that the magmas intruded stocks or batholiths in the shallow crust, permitting magmatic differentiation and assimilation of volatiles from the surrounding country rock.

Eleven stage 1 volcanoes (unit Nfu; Fig. 2) occur in the Coprates, Thaumasia Highlands, Daedalia Planum, and Terra Sirenum provinces. Several smaller domes in the Coprates and Thaumasia Highland provinces (Fig. 2) may also be volcanoes formed during this time. Local volcanism likely contributed to the formation of outcrops of stage 1 plateau materials as well, but such outcrops cannot be isolated with present data.

During stage 2, volcanism produced three volcanoes (unit HNfu; Fig. 2) in the Thaumasia Highlands province. Also during this time, widespread volcanism likely continued to resurface local areas throughout the map region. In particular, plains volcanism produced older ridged plains material (unit HNr) in the Thaumasia Planum and northwestern part of the Argyre provinces. Troughed material (unit HNplt) may be pyroclastic material that was deposited in the southern part of Coprates province (Schultz and Tanaka, 1994). Younger rocks probably bury older ridged plains material in places; for example, subdued ridges in Daedalia Southeast province may be raised outcrops of otherwise buried older ridged plains material.

The Hesperian records extensive volcanic plains emplacement across the interior of the Thaumasia plateau and in Daedalia Planum. Stage 3 younger ridged plains material (unit Hr; Fig. 2) in the Sinai Planum and Coprates East provinces onlaps older ridged plains material in Thaumasia Planum (unit HNr). Stages 3 and 4 sheet lavas (units Ht_{1-2}, Hsl_{1-2} and Hsu) cover the Syria-Solis, Daedalia Planum, and Daedalia Southeast provinces and were erupted from the crest and flanks of Syria Planum and Arsia Mons (outside study area at lat. 10°S, long. 120°). Continued Tharsis volcanic activity during the Amazonian (stage 5) resulted in the emplacement of lava flows in the Daedalia Planum province (units AHt_3 and At_5).

6. Erosional history

We have mapped and dated > 4000 single and branching valleys (Fig. 4), using the same basic stratigraphic principles and methods as used for the tectonic structures. Branching, or networked, valleys strongly indicate water- or ice-based erosion, whereas single, nonbranching valleys may also form by eolian, tectonic, and (or) volcanic processes. Although we excluded likely volcanic rilles and narrow grabens, many of the single valleys may have originated as such and then later were modified by fluvial or other erosional processes.

6.1. Regional valley development

Overall, valley formation in the Thaumasia region was most extensive during stages 1 and 2 (Fig. 4 and Table 5). Valleys tend to concentrate in certain areas, including volcano flanks and near rift systems of the central part of the Thaumasia Highlands province and southern part of the Coprates province. Elsewhere, minor numbers of individual or small groups of single valleys and valley networks are dispersed unevenly throughout stage 1 and 2 rocks. Particularly devoid of valleys is the relatively flat and resistant older ridged plains material (unit HNr). Commonly, stage 1 valleys are obscure and discontinuous, probably due to later resurfacing (Baker and Partridge, 1986). Stages 3 and 4 valleys tend to be more pristine and mostly occur near rifts or large craters. No stage 5 valleys occur in the map region. These broad findings are in general agreement with the results of global but less detailed studies of highland valley spatial and temporal distribution (Carr, 1995; Scott et al., 1995; Carr and Chuang, 1997).

The Argyre province portrays a particularly complex erosional history during the Noachian and Hesperian. Valley networks and single valleys dissected a number of isolated drainage basins that are not evidently associated with volcanoes and highly faulted terrains, as in the Thaumasia Highlands, although large impact craters are abundant in the province. In addition, stage 2 resurfacing formed or modified large troughs, irregular depressions, and subtle ridges. These eroded areas are mapped as dissected and etched material (unit HNade, Fig. 2). This variety in landforms in the Argyre province may largely be due to the complex, irregular topography generated by the impact. Additionally, a variety of processes including eolian, mass-wasting, sapping, fluvial, and glacial processes (Baker et al., 1991; Kargel and Strom, 1992) and (or) hydrothermal activity related to basin-controlled intrusions (Schultz et al., 1982) may have contributed to the diversity of landforms.

During stage 3, valley formation declined substantially and was concentrated in a few places along the south and southeast margins of the Thaumasia Highlands and Coprates provinces, near rifts and two large impact craters of similar age (sites 7 and 9 in Fig. 13). For the craters, relatively pristine, single or moderately branching valleys occur downslope from them and in some cases originate within stages 1–3 grabens. The craters are Lampland (70

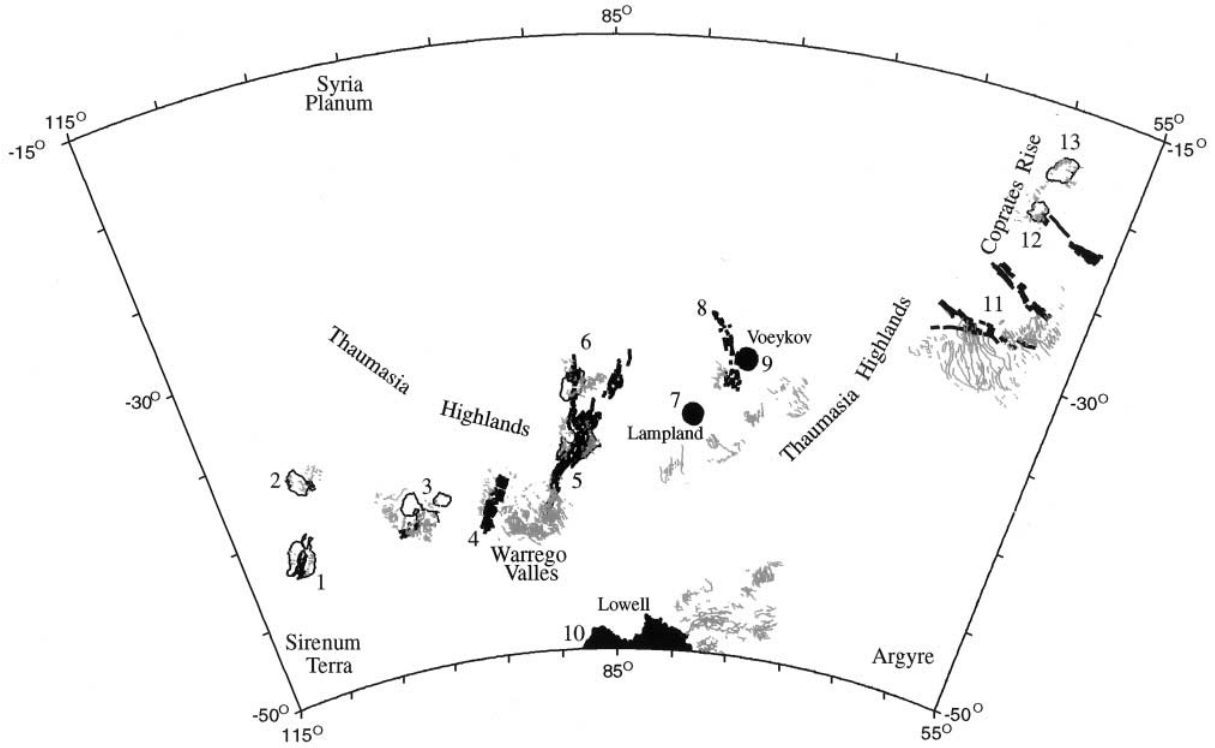

Fig. 13. Thirteen candidate hydrothermal sites of Thaumasia, showing associated channels (gray lines), volcanoes (black outlines), rifts (black lines), and craters (black areas). See Table 6 for explanations of individual sites.

km diameter; 36.0°S, long. 79.5°), whose ejecta onlaps stage 3 smooth plateau material (unit Hpl_3), and Voeykov (75 km diameter; lat. 32.5°S, long. 76°). For stage 4, valley development in the map region was restricted to an area 100–350 km northeast of the double-ring, 195-km-diameter Lowell impact crater (Lias et al., 1997). There, dense, locally degraded networks of valleys cut dissected and etched plains (unit HNade). Other similar valley networks occur 150–300 km southwest of Lowell (outside the map area). Detailed crater statistics indicate that both sets of valleys formed during the Late Hesperian/Early Amazonian (stage 4), perhaps coincident with the Lowell impact event (Lias et al., 1997).

Valleys of the southern part of the Coprates rise have a somewhat different morphology than those in other areas. Here, the valleys have broad, gently sloping walls. To distinguish these valleys, we refer to them as troughs. The troughs originate from stage 2 faults that form large irregular depressions along the southern edge of the older ridged plains materials (unit HNr of Fig. 2) and from a large scarp that may have formed by tectonic activity associated with the development of Coprates rise (site 11, Figs 8 and 13). The valleys cut both stage 2 and 3 materials, and thus are assigned the same ages. However, all of the dissection could have occurred during stage 3. The troughs resemble the valleys that dissect the flanks of Tyrrhena and Hadriaca Paterae elsewhere on Mars (Greeley and Crown, 1990; Gulick and Baker, 1990; Crown and Greeley, 1993) and eroded ignimbrites on Earth (Dohm et al., in press). Thus, the eroded rock outcrops, mapped as troughed material (unit HNplt), may be pyroclastic deposits, perhaps erupted in part from gaping fissures occurring in higher elevation areas of the unit. Many of the troughs head near faults and large depressions, indicating that release of ground water likely occurred along fractures, perhaps in association with magmatic activity. The process linkage may be similar to that proposed for the Elysium and Galaxias regions of Mars where ground-ice melting due to volcanism may have resulted in valley systems (Baker, 1982; Mouginis-Mark et al., 1984; Mouginis-Mark, 1985). Alternatively, faulting may have disrupted impermeable, frozen rock, providing conduits for the release of water from otherwise confined aquifers (MacKinnon and Tanaka, 1989).

In many areas of Thaumasia, crosscutting relations among valleys, structures, and geologic units indicate that dissection appears to be limited to one episode. However, in the Warrego Valles region, valley development consisted of at least two distinct episodes (see Fig. 4 and site 4 in Figs 8 and 13). During stage 1, a pair of north-trending rifts flanking the mountains above the site of Warrego were initiated, with some valley development occurring along the western rift. As rift development continued and perhaps peaked during stage 2, the majority of the Warrego Valles dissection, on the southern slope of the interrift mountains, took place. A large

depression and pit crater chains within the floor of the western rift system (site 4 in Fig. 13) indicate relatively young, possible stage 3 collapse. Heading at the eastern rift system and just northeast of Warrego Valles, another well-integrated valley network system was carved into the mountain slopes. The later, stages 2 and 3, valley systems dissect Noachian and Early Hesperian brecciated rock materials and modify and destroy stages 1 and 2 fault systems.

7. Discussion

Here we discuss topical problems regarding the Thaumasia region for which previous analysis has been lacking or meager. Our detailed geologic studies provide a basis to address tectonic, magmatic, and resurfacing issues in greater depth.

7.1. Thaumasia plateau development

The Thaumasia plateau is unique to Mars in terms of its size, elevation, and structural character. During stages 1 and 2, the Thaumasia plateau appears to have formed largely by uplift, producing possible outward-verging fold-and-thrust margins and systems of narrow grabens and rifts (Schultz and Tanaka, 1994). The margins of the plateau in the Coprates and Thaumasia Highlands provinces are marked by tilted and possibly folded strata, mountain ranges, volcanoes, broad ridges, large scarps, wrinkle ridges, and fault and rift systems (Figs 8 and 14A). Many of the linear ridges and scarps have been previously interpreted as contractional folds or thrust faults (Plescia et al., 1980; Saunders et al., 1980; Watters, 1993; Schultz and Tanaka, 1994; Dohm et al., in press).

What caused the plateau uplift? Mechanisms to consider include (1) plate tectonics, which dominates plateau development and ridge-belt formation on Earth, and (2) mantle upwelling and (or) downwelling, which appears to dominate on Venus. One way we can address the cause of plateau uplift is to compare the structures and lithospheric character associated with Thaumasia plateau development to those of plateaus on Earth and Venus.

The simple geometry of the contractional structures along the southern and eastern margins of the plateau differs from most fold mountains on Earth and Venus. Terrestrial fold geometries generally consist either of a broad series of folds of similar wavelength and amplitude or of disharmonic, perhaps overlapping, folds. Such fold belts are common along continental plate boundaries (e.g., LePichon et al., 1973; Suppe, 1985). On Venus, where the lithosphere is relatively thin and the tectonic record presumably has been controlled by mantle plumes leading to mantle upwelling and downwelling, belts of regular folds characterize much of its highlands and parts of its plains (e.g., Hansen et al., 1997).

Instead, the structural style of the Thaumasia plateau is comparable to that of some intracontinental plateaus and mountain ranges on Earth. One example is the younger ranges of the Rocky Mountains in the western United States. Deep crustal roots, contractional and extensional deformation, and valley dissection of their margins characterize both the Thaumasia Plateau and Rocky Mountains. For example, both the Coprates rise and the Wind River Mountain Range appear to be asymmetric anticlines, and each displays cuestas, hogbacks, faults, and erosional valleys (Fig. 14). Coprates is about 900 km long and 2–4 km high, or approximately twice the size of the Wind River Mountain Range. The Coprates rise is the largest of several probably contractional features that form the south Tharsis ridge belt, which rings the east, south, and southwest margins of the Thaumasia plateau and the west margin of Daedalia Planum (Schultz and Tanaka, 1994).

Fold-and-thrust structures that bound many of the ranges of the Rocky Mountains provide unequivocal evidence for horizontal crustal shortening in foreland areas (Blackstone, 1980, 1983; Berg, 1981; Kanter et al., 1981). However, mantle-driven differential vertical movements may explain the 5–9 km of structural relief between the foreland uplifts and adjoining basins (Woodward, 1976; Stearns, 1978). Some of the mountain ranges include batholiths that consist of multiple intrusions over time. Other terrestrial examples of regional uplift, which may include related magmatic activity and thermal rise, are the Colorado Plateau in the western United States (Pierce et al., 1978, 1979; Lucchitta, 1979; Young, 1979), the Rhenish shield in Germany (Illies et al., 1979), and the Deccan and Karnataka Plateaus of the southern peninsular shield in India (Kailasam, 1979). The aggregation of tectonic and volcanic features, high topography, thick crust, and possible hydrothermal valleys along the margins of the Thaumasia plateau also may result from prolonged intrusive activity (Tanaka et al., 1998). The crust beneath the Thaumasia plateau may be up to 120 km thick—about 40 km thicker than the estimated mean crustal thickness for the rest of the martian cratered highlands (Frey, personal communication, 1996). This great thickness may have been achieved by crustal underplating. In the scenario proposed by Wise et al. (1979), mantle convection causes subcrustal erosion beneath the northern plains. The eroded material is intruded into the base of the crust—in this case beneath the Thaumasia plateau. The low-density root results in rapid, permanent uplift.

Regional uplift of the Thaumasia plateau apparently contributed to thrusting and folding and rifting and graben development in rocks along the margins of the plateau (Fig. 8). Generally, contractional features are oriented parallel with the plateau margins, and extensional features are oblique or perpendicular (Fig. 3). The rift systems of Thaumasia are defined by long, tens-of-

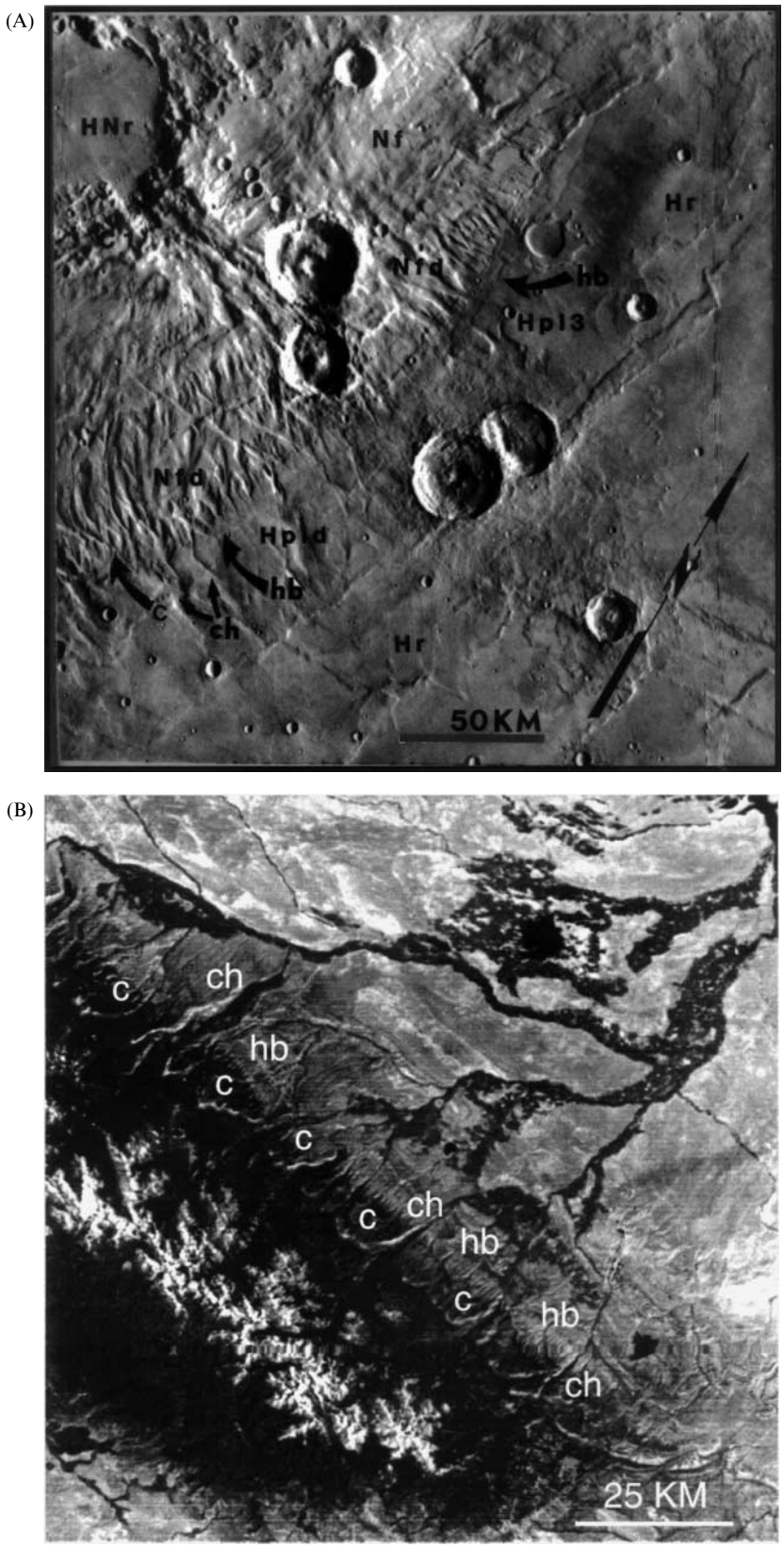

Fig. 14. (A) Southeast part of Coprates rise, Mars, showing cuestas (c), hogbacks (hb), and channels (ch) formed by tectonic tilting and differential erosion of rock strata. Geologic units include older fractured material (unit Nf), fractured and dissected material (unit Nfd), older and younger ridged plains materials (units HNr and Hr, respectively), smooth unit of the plateau sequence (unit Hpl_3), and younger dissected material (unit Hpld) [Viking image 610A44; resolution 224 m/pixel] (B) Wind River Mountain Range of the Rocky Mountains in Wyoming, U.S., that display cuestas (c), hogbacks (hb) and channels (ch) similar to those of the Coprates rise. [Landsat TM image.]

kilometers-wide, relatively deep grabens and associated narrow fractures and grabens. In some cases, the rifts include irregular depressions probably formed by collapse, perhaps associated with magma withdrawal, and volcanic constructs (Fig. 8). All these tectonic and volcanic features overlap in age, forming episodically during stages 1 and 2. These temporal and spatial associations are consistent with a scenario in which crustal underplating leads to uplift of the Thaumasia plateau and emplacement of shallow crustal batholiths, over which rifting, volcanism, and hydrothermal activity occur (more discussion on intrusion below).

Given that Valles Marineris forms the northern boundary of the Thaumasia plateau, another mechanism for plateau development could be plate tectonics, in which extension within the troughs was accommodated by contraction on the Thaumasia plateau margin. However, this scenario appears to conflict with a variety of observations, including: (1) the eastern and western margins of the Thaumasia plateau are perpendicular to the Valles Marineris, (2) comparable contractional structures north of Valles Marineris do not occur, and (3) Valles Marineris appears to have been highly active during the Late Hesperian, then diminishing into the Amazonian (Schultz, 1991; Witbeck et al., 1991), but Thaumasia uplift shut down during the Early Hesperian.

7.2. Valley origins

In a related study, we demonstrate that sources of valleys in the Thaumasia region largely occur near volcanoes, highly faulted terrains, and large (>50 km in diameter) impact craters of similar age (Tanaka et al., 1998). These associations are strongest for stages 1–3, when most activity occurred. Presumably, impacts produce shallow hydrothermal systems (Brakenridge et al., 1985) and may seismically fluidize water-saturated rocks and cause outbreaks of ground water (Clifford, 1993). Volcanoes and rifts may overlie magmatic intrusions, leading to long-lived hydrothermal systems and surface runoff of thermal water or melted snows (Gulick and Baker, 1990; Gulick et al., 1997; Gulick, 1998). After stage 2, when the martian cryosphere may have thickened to more than a kilometer, some local sets of valleys that formed may be related to the impact of two large craters in the Thaumasia Highlands province and to Lowell crater at the south-central edge of the map area (Fig. 13). Widespread, heavy precipitation was not likely a primary factor in valley formation in most of the Thamasia region, except perhaps during the Early Noachian, for which much of the geologic record has been destroyed.

We propose 13 sites of concentrated valley formation associated with possible magmatic intrusions and large impact craters within the Thaumasia region (Fig. 13; Table 6). These are the best examples of valleys associated with geologic features, but there are other less pronounced correlations elsewhere in the region. Such sites will require further evaluation for hydrothermal activity; for example, if they produced zones of mineral alteration, they may have distinctive spectral signatures in TES data (Christensen et al., 1998).

7.3. Intrusions beneath the Thaumasia plateau

Since crustal magmatic intrusions cannot be detected directly on Mars, their existence must be inferred from surface geology (e.g., Scott and Dohm, 1990c). Generally, large intrusions may develop beneath or near rifts and volcanoes. Three prime candidate sites for intrusive activity in the Thaumasia region include (1) Warrego Valles, and the topographic rise they cut, (2) the source areas of the volcano-rift complex situated along the southwest part of the plateau, and (3) large networking troughs of the troughed material (unit HNplt of Fig. 2) of southern Coprates rise (sites 3, 4, 11 in Figs 8 and 13). These sites include coeval rifts, apparent volcanic vents, well-developed valley network systems, and local depressions and pit chains commonly aligned with the trend of the rifts. These associations suggest that the valleys were largely a result of hydrothermal circulation of ground water related to intrusion (Gulick, 1998; Gulick et al., 1998; Tanaka et al., 1998).

Additionally, Warrego's source area forms a pronounced topographic high nestled between the southern parts of two rift systems (Figs 8 and 13). Intrusion may have occurred during stages 1 and 2, leading to rifting and valley dissection (Dohm et al., 1998). Also, stage 3 faults of southern Claritas Fossae diverge or terminate as they approach the Warrego source area, perhaps due to greater resistance to extensional faulting afforded by an intrusive body. Finally, fault-intersection data for the martian western equatorial region indicate that the Warrego source area is a local center of stage 2 tectonic activity (Anderson et al., 1998). Thus, intrusions may provide strong regional control on fault orientations. Modeling results (Gulick, 1998; Gulick et al., 1998) also indicate that Warrego may have formed as a result of magmatic-related hydrothermal activity. This valley system is one of the most well-developed on Mars and has commonly been cited as a potential indicator of an early warm and wet climate.

7.4. Syria Planum volcanotectonic development

Similar to and perhaps associated with long-lived Tharsis-centered activity, the corona-like feature of Syria Planum may have developed over much of martian geologic history. The wide age range of Syria-centered faults and probably lava units from the Middle Noachian to the end of the Hesperian (stages 1–4; Fig. 7) demonstrate long-lived volcanotectonic activity at Syria Planum, especially in the Syria-Solis and Thaumasia Highlands

Table 6
Local sites of valley formation in the Thaumasia region of Mars. Possible causes of formation include magmatic intrusions that led to hydrothermal activity, perhaps augmented by local precipitation, and impact-induced ground-water heating, seismic fluidization, and ground-water outbreaks. Site locations shown in Fig. 14

Site	Geologic features suggestive of valley origin	Valley origin	Stage
1	Volcano, faults and grabens, rift system	Intrusion	1
2	Volcano, lava flows, contractional ridges and scarps, faults and grabens	Intrusion	2
3	Volcano, lava flows, rift system, faults and grabens, large scarps	Intrusion	2
4	High topography, large depression, deflected faults and grabens near Warrego Valles source region, pit chains, rift system, faults and grabens, contractional ridges and scarps	Intrusion	2–3
5	Volcano, rift systems, faults and grabens, contractional scarps	Intrusion	2
6	Volcano, rift systems, faults and grabens	Intrusion	1
7	Lampland crater, faults and grabens, contractional ridges and scarps	Impact	2–3
8	Rift systems, faults and grabens, contractional ridges	Intrusion	1
9	Voeykov crater, faults and grabens, contractional ridges and scarps	Impact	2–3
10	Lowell crater	Impact	4
11	Rift systems, faults and grabens, depressions (near source regions), contractional scarps, subdued wrinkle ridges, possible pyroclastic deposit	Intrusion	2–3
12	Volcano, rift system, faults and grabens	Intrusion	1
13	Volcano, faults and grabens	Intrusion	1

provinces. In particular, an exceptional east-to-west sequence of lava-flow units occurs across the western interior of the Thaumasia plateau from Sinai and Solis Plana to Syria Planum. If the stages 2 and 3 ridged plains materials (units HNr and Hr) in the Sinai Planum and Thaumasia Planum provinces also originated from the Syria Planum region, the age progression would be from Late Noachian to Late Hesperian. In addition, unit morphology changes from smooth, broad, thin flows of the ridged plains materials to rugged, thick, irregular lobate flows of the Syria Planum Formation. Syria Planum may have also been the source of older stage 1 and 2 lavas that form older deformed plains materials (units Nf and HNf) of northern Claritas Fossae and Noctis Fossae (north of Syria Planum).

7.5. Thaumasia and Tharsis evolution

Thaumasia volcanotectonic activity occurred during an early phase of Tharsis development (Plescia and Sanders, 1982; Tanaka et al., 1991). Activity centered at Syria Planum may have begun early in the development of Thaumasia and of Tharsis as a whole, with the development of some concentrically oriented fault scarps of Claritas Fossae in some of the oldest rocks in the region (Tanaka and Davis, 1988). These faults may have been produced by early flexural doming of Tharsis (Phillips et al., 1990). Most faults formed later, including narrow radiating grabens near the center of Tharsis and peripheral, concentric wrinkle ridges. These features formed contemporaneously and may be consistent with the mechanical behavior of an intrusively thickened crust (Tanaka et al., 1991). If evaluated in terms of fault-intersection densities (Watters, 1993; Anderson et al., 1997, 1998), Syria Planum and the Tharsis Montes, particularly Pavonis Mons, define the overall center for Tharsis stress and strain. Thus the Thaumasia plateau is in large part a peripheral center of Tharsis activity, similar to Valles Marineris, Tempe Terra, Alba Patera, Acheron Fossae, and Olympus Mons as portrayed by Tanaka et al. (1991). Each of these various regions appear to have been active over shorter durations relative to the Syria-Tharsis regional center and to have developed distinctive volcanotectonic structures and histories.

8. Summary

This summary provides an interpretive geologic history of the Thaumasia region based on our geologic mapping and topical analyses.

8.1. Early to Middle Noachian, stage 1

Ancient crustal rocks were emplaced during a period of waning intense bombardment that produced a high density of large impact craters and the enormous Argyre basin. The Thaumasia Highlands began to rise as a result of crustal underplating and intrusive thickening. This process formed marginal fold and thrust structures where the edge of the emerging plateau pushed over foreland areas. In addition, volcanoes, broad ridges and scarps, and rifts began to form on the plateau as a result of local intrusions. Regional faulting produced sets of narrow grabens radial to Tharsis, Syria Planum, and perhaps Valles Marineris; a few fault scarps formed concentric to Syria Planum in Claritas Fossae. Middle Noachian valleys

show concentrations near volcanoes, rifts, and large impact craters.

8.2. Late Noachian, stages 1 and 2

Widespread resurfacing during this time subdued and degraded pre-existing units and structures. Locally, intercrater deposits were deposited and older ridged plains material covered Thaumasia Planum province. Continued rise of the Thaumasia plateau, Tharsis volcanotectonic development, and local intrusive activity led to further volcanism, graben and wrinkle-ridge formation, and valley dissection. Along the northern margin of the Thaumasia plateau, incipient rifting of Valles Marineris began. Some of the narrow grabens in the Thaumasia region radiate from centers of tectonic activity at Valles Marineris and the topographic high dissected by Warrego Valles. As in stage 1, valleys developed particularly near rifts and volcanoes, whereas others formed scattered about in local basins such as in the rim of Argyre basin. The valley associations with rifts, volcanoes, and impact craters suggest that valleys originated from hydrothermal and seismic processes. Snowpacks may have contributed to runoff in areas where geothermal heating was intense.

8.3. Early Hesperian, stages 2 and 3

Lavas and sediments formed patches of smooth deposits in areas scattered about the Thaumasia Highlands and other cratered terrains bordering the Thaumasia plateau. Widespread tectonic deformation produced wrinkle ridges, narrow grabens, and other structures. Narrow grabens radial to Tharsis continued to form a Claritas and Thaumasia Fossae. Further rifting and ridged plains volcanism occurred at Valles Marineris. Local valley systems developed along the southern and southeastern margins of the Thaumasia plateau in association with possible intrusions such as beneath a rift near Warrego Valles and downslope from two large impact craters, perhaps due to seismic fluidization and expulsion of water from confined aquifers.

8.4. Late Hesperian, stage 4

Extensive lobate flows were emplaced in the Syria-Solis, Daedalia Planum, and Daedalia Southeast provinces from the summit areas and flanks of Tharsis Montes volcanoes and Syria Planum. Meanwhile, formation of Tharsis-radial narrow grabens declined substantially. Valles Marineris rifting likely peaked at this time. Lowell impact formed, generating extensive valley systems in nearby rocks.

8.5. Amazonian, stage 5

Geologic activity was greatly reduced in the Thaumasia region. Lobate flows were effused from Arsia Mons and emplaced in Daedalia Planum. Minor Tharsis-radial faults formed in the northwest corner of map region. No valleys were dissected; local wind erosion and deposition became the dominant forms of resurfacing.

Acknowledgments

We thank Trent Hare and Juan Lias (USGS) for help with gathering statistical data used in this paper. Nathalie Cabrol, Virginia Gulick, Jeff Johnson, and Jeff Kargel provided reviews that greatly improved the manuscript.

References

Anderson, R.C., Golombek, M.P., Franklin, B.J., Tanaka, K.L., Dohm, J.M., Lias, J., Higdon, J., 1997. A new detailed structural history of the Thaumasia region of Mars. Lunar Planet. Sci. XXVIII, 39–40.

Anderson, R.C., Golombek, M.P., Franklin, B.J., Tanaka, K.L., Dohm, J.M., Lias, J.H., Peer, B., 1998. Centers of tectonic activity through time for the western hemisphere of Mars. Lunar and Planet. Sci. XXIX, 1881.

Baker, V.R., 1982. The Channels of Mars. University of Texas Press, Austin.

Baker, V.R., Partridge, J., 1986. Small Martian valleys: pristine and degraded morphology. J. Geophys. Res. 91, 3561–3572.

Baker, V.R., Strom, R.G., Gulick, V.C., Kargel, J.S., Komatsu, G., Kale, V.S., 1991. Ancient oceans, ice sheets and the hydrological cycle on Mars. Nature 352, 589–594.

Berg, R.R., 1981. Review of thrusting in the Wyoming foreland. In: Boyd, D.W., Lillegraven, J.A. (Eds.), University of Wyoming Contributions to Geology, 19, 93–104.

Blackstone Jr., D.L., 1980. Foreland deformation: compression as a cause. In: University of Wyoming Contributions to Geology, 18, 83–100.

Blackstone Jr., D.L., 1983. Laramide compressional tectonics, southeastern Wyoming. In: University of Wyoming Contributions to Geology, 22, 1–38.

Brakenridge, G.R., Newsom, H.E., Baker, V.R., 1985. Ancient hot springs on Mars: origins and paleoenvironmental significance of small Martian valleys. Geology 13, 859–862.

Carr, M.H., 1995. The martian drainage system and the origin of valley networks and fretted channels. J. Geophys. Res. 100 (E4), 7479–7507.

Carr, M.H., Chuang, F.C., 1997. Martian drainage densities. J. Geophys. Res. 102 (E4), 9145–9152.

Christenson, P.R., Anderson, D.L., Chase, S.C., Clancy, R.T., Clark, R.N., Conrath, B.J., Kieffer, H.H., Kuzmin, R.O., Malin, M.C., Pearl, J.C., Roush, T.L., Smith, M.D., 1998. Results from the Mars Global Surveyor Thermal Emission Spectrometer. Science 279, 1692–1698.

Clifford, S.M., 1993. A model for the hydrologic and climate behavior of water on Mars. J. Geophys. Res. 98, 10,973–11,016.

Craddock, R.A., Greeley, R., Christensen, P.R., 1990. Evidence of an ancient impact basin in Daedalia Planum, Mars. J. Geophys. Res. 95, 10,729–10,740.

Crown, D.A., Greeley, R., 1993. Volcanic geology of Hadriaca Patera

and the eastern Hellas region of Mars. J. Geophys. Res. 98, 3431–3451.
Dohm, J.M., Anderson, R.C., Tanaka, K.L., 1998. Digital structural mapping of Mars. Astronomy and Geophysics 39, 3.20–3.22.
Dohm, J.M., Tanaka, K.L., Hare, T.M., 1999. Geologic, paleotectonic, and paleoerosional maps of the Thaumasia region, Mars (1 : 5,000,000). USGS Misc. Inv. Ser. Map I-2650, in press.
Golombek, M.P., Franklin, B.J., Tanaka, K.L., Dohm, J.M., 1997. Extension through time across Thaumasia, Mars. Lunar Planet. Sci. XXVIII, 431–432.
Greeley, R., Crown, D.A., 1990. Volcanic geology of Tyrrhena Patera, Mars. J. Geophys. Res. 95, 7133–7149.
Greeley, R., Spudis, P.D., 1981. Volcanism on Mars. Geophys. Space Phys. Rev. 19, 13–41.
Gulick, V.C., 1998. Magmatic intrusions and a hydrothermal origin for fluvial valleys on Mars. J. Geophys. Res. 103 (E8), 19,365–19,387.
Gulick, V.C., Baker, V.R., 1990. Origin and evolution of valleys on Martian volcanoes. J. Geophys. Res. 95 (9), 14,325–14,344.
Gulick, V.C., Tyler, D., McKay, C.P., Haberle, R.M., 1997. Episodic ocean-induced CO_2 pulses on Mars: implications for fluvial valley formation. Icarus 130, 68–86.
Gulick, V.C., Dohm, J.M., Tanaka, K.L., Hare, T.M., 1998. The origin of Warrego Valles: a case study for fluvial valley formation on early Mars. Lunar and Planet. Sci. XXIX, 1933.
Hansen, V.L., Willis, J.J., Banerdt, W.B., 1997. Tectonic overview and synthesis. In: Bougher et al. (Eds.), Venus II. University of Arizona Press, Tucson, pp. 797–844.
Hodges, C.A., Moore, H.J., 1994. Atlas of volcanic landforms on Mars. USGS Prof. Paper 1534.
Illies, J.H., Prodehl, C., Schmincke, H., 1979. The Quaternary uplift of the Rhenish shield in Germany. Tectonophysics 61, 197–225.
Kailasam, L.N., 1979. Plateau uplift in Peninsular India. Tectonophysics 61, 243–269.
Kanter, L.R., Dyer, R., Dohmen, T.E., 1981. Laramide crustal shortening in the northern Wyoming province. In: Boyd, D.W., Lillegraven, J.A. (Eds.), University of Wyoming Contributions to Geology, 19, 135–142.
Kargel, J.S., Strom, R.G., 1992. Ancient glaciation on Mars. Geology 20, 3–7.
LePichon, X., Francheteau, J., Bonnin, J., 1973. Plate Tectonics. Elsevier, New York.
Lias, J.H., Dohm, J.M., Tanaka, K.L., 1997. Geologic history of Lowell impact. Lunar Planet. Sci. XXVIII, 813–814.
Lucchitta, I., 1979. Late Cenozoic uplift of the southwestern Colorado plateau and adjacent lower Colorado river region. Tectonophysics 61, 63–95.
MacKinnon, D.J., Tanaka, K.L., 1989. The impacted martian crust: structure, hydrology, and some geologic implications. J. Geophys. Res. 94 (B12), 17,359–17,370.
Morris, E.M., Tanaka, K.L., 1994. Geologic maps of the Olympus Mons region of Mars (1 : 1,000,000 and 1 : 2,000,000). USGS Misc. Inv. Ser. Map I-2327.
Mouginis-Mark, P.J., 1985. Volcano/ground ice interactions in Elysium Planitia, Mars. Icarus 64 (2) part 1, 265–284.
Mouginis-Mark, P.J., Wilson, L., Head, J.W., 1982. Explosive volcanism on Hecates Tholus, Mars: investigation of eruptive conditions. J. Geophys. Res. 87, 9890–9904.
Mouginis-Mar, P.J., Wilson, L., Head, J.W., Brown, S.H., Hall J.L., Sullivan, K.D., 1984. Elysium Planitia, Mars: regional geology, volcanology, and evidence for volcano–ground ice interactions. Earth, Moon, and Planets 30, 149–173.
Phillips, R.J., Sleep, N.H., Banerdt, W.B., 1990. Permanent uplift in magmatic systems with application to the Tharsis region of Mars. J. Geophys. Res. 95, 5089–5100.
Pierce, H.W., Damon, P.E., Shafiqullah, M., 1978. Plateau uplift in Arizona—a conceptual review. In: Plateau Uplift: Mode and Mechanism. Lunar and Planetary Institute, Houston, pp. 37–39.
Pierce, H.W., Damon, P.E., Shafiqullah, M., 1979. An Oligocene (?) Colorado Plateau edge in Arizona. Tectonophysics 61, 1–24.
Plescia, J.B., Saunders, R.S., 1979. The chronology of the Martian volcanoes. In: Proc. Lunar Planet. Sci. Conf. 10, 2841–2859.
Plescia, J.B., Saunders, R.S., 1982. Tectonic history of the Tharsis region, Mars. J. Geophys. Res. 87, 9775–9791.
Plescia, J.B., Roth, L.E., Saunders, R.S., 1980. Tectonic features of southeast Tharsis. In: Reports of Planetary Geology Program. NASA Tech. Memo. 81,776, pp. 68–70.
Reimers, C.E., Komar, P.D., 1979. Evidence for explosive density currents on certain Martian volcanoes. Icarus 39, 88–110.
Robinson, M.S., Mouginis-Mark, P.J., Zimbelman, J.R., Wu, S.S.C., Ablin, K.K., Howington-Kraus, A/E., 1993. Chronology, eruption duration, and atmospheric contribution of the Martian volcano Apollinaris Patera. Icarus 104, 301–323.
Saunders, R.S., Roth, L.E., Downs, G.S., Schubert, G., 1980. Early volcanic–tectonic province: Coprates region of Mars. In: Reports of Planetary Geology Program. NASA Tech. Memo. 81,776, pp. 74–75.
Schultz, R.A., 1991. Structural development of Coprates Chasm and western Ophir Planum, Valles Marineris rift, Mars. J. Geophys. Res. 96, 22,777–22,792.
Schultz, R.A., Tanaka, K.L., 1994. Lithospheric-scale buckling and thrust structures on Mars: the Coprates rise and south Tharsis ridge belt. J. Geophys. Res. 99, 8371–8385.
Schultz, P.H., Schultz, R.A., Rogers, J., 1982. The structure and evolution of ancient impact basins on Mars. J. Geophys. Res. 87 (B12), 9803–9820.
Scott, D.H., 1982. Volcanoes and volcanic provinces: Martian western Hemisphere. J. Geophys. Res. 87, 9839–9851.
Scott, D.H., Dohm, J.M., 1990a. Chronology and global distribution of fault and ridge systems on Mars. In: Proc. Lunar Planet. Sci. Conf. 20, 487–501.
Scott, D.H., Dohm, J.M., 1990b. Faults and ridges: historical development in Tempe Terra and Ulysses Patera regions of Mars. In: Proc. Lunar Planet. Sci. Conf. 20, 503–513.
Scott, D.H., Dohm, J.M., 1990c. Tectonic setting of Martian volcanoes and deep-seated intrusives. In: MEVTV Workshop "Evolution on Magma Bodies on Mars". LPI Tech. Rep. 90-04, pp. 39–40.
Scott, D.H., King, J.S., 1984. Ancient surfaces of Mars: the basement complex. Lunar Planet. Sci. XV, 736–737.
Scott, D.H., Tanaka, K.L., 1980. Mars Tharsis region: volcanotectonic events in the stratigraphic record. In: Proc. Lunar Planet. Sci. Conf. 11, 2403–2421.
Scott, D.H., Tanaka, K.L., 1981. Mars: a large highland volcanic province revealed by Viking images. In: Proc. Lunar Planet. Sci. Conf. 12, 1449–1458.
Scott, D.H., Tanaka, K.L., 1986. Geologic map of the western equatorial region of Mars (1 : 15,000,000). USGS Misc. Inv. Ser. Map I-1802-A.
Scott, D.H., Dohm, J.M., Rice Jr., J.W. 1995. Map of Mars showing channels and possible paleolake basins. USGS Misc. Inv. Ser. Map I-2461.
Stearns, D.W., 1978. Faulting and folding in the Rocky Mountain foreland. In: Matthews, V.I. (Ed.), Laramide Folding Associated with Basement Block Faulting in the Western United States. Geol. Soc. of America Mem. 151, pp. 1–37.
Suppe, J., 1985. Principles of Structural Geology. Prentice-Hall.
Tanaka, K.L., 1986. The stratigraphy of Mars. J. Geophys. Res. 91, E139–E158.
Tanaka, K.L., 1990. Tectonic history of the Alba Patera–Ceraunius Fossae region of Mars. In: Proc. Lunar Planet. Sci. Conf. 20, 515–523.
Tanaka, K.L., Davis, P.A., 1988. Tectonic history of the Syria Planum province of Mars. J. Geophys. Res. 93 (B12), 14,893–14,917.
Tanaka, K.L., Golombek, M.P., Banerdt, W.B., 1991. Reconciliation

of stress and structural histories of the Tharsis region of Mars. J. Geophys. Res. 96, 15,617–15,633.

Tanaka, K.L., Dohm, J.M., Watters, T.R., 1996. Possible coronae structures in the Tharsis region of Mars. Lunar Planet. Sci. XXVII, 1315–1316.

Tanaka, K.L., Dohm, J.M., Lias, J.H., Hare, T.M., 1998. Erosional valleys in the Thaumasia region of Mars: hydrothermal and seismic origins. J. Geophys. Res., in press.

Thomas, P.G., Masson, P., 1984. Geology and tectonics of the Argyre area on Mars: comparisons with other basins in the solar system. Earth, Moon, and Planets 31, 25–42.

U.S. Geological Survey, 1989. Topographic maps of the western, eastern equatorial, and polar regions of Mars (1 : 15,000,000). USGS Misc. Inv. Ser. Map I-2030.

Watters, T.R., 1993. Compressional tectonism on Mars. J. Geophys. Res. 98 (E9), 17,049–17,060.

Wichman, R.W., Schultz, P.H., 1989. Sequence and mechanisms of deformation around the Hellas and Isidis impact basins on Mars. J. Geophys. Res. 94, 17,333–17,357.

Wise, D.U., Golombek, M.P., McGill, G.E., 1979. Tharsis province of Mars: geologic sequence, geometry, and a deformation mechanism. Icarus 38 (3), 456–472.

Witbeck, N.E., Tanaka, K.L., Scott, D.H., 1991. Geologic map of the Valles Marineris region, Mars (east half and west half; 1 : 2,000,000). USGS Misc. Inv. Ser. Map I-2010.

Woodward, L.A., 1976. Laramide deformation of Rocky Mountain foreland: geometry and mechanics. In: Woodward, L.A., Northrop, S.A. (Eds.), Tectonics and mineral resources of southwestern North America. New Mexico Geol. Soc. Spec. Pub. No. 6, pp. 11–17.

Young, R.A., 1979. Laramide deformation, erosion and plutonism along the southwestern margin of the Colorado Plateau. Tectonophysics 61, 25–47.